

Correlation functions of the integrable $SU(n)$ spin chain

G.A.P. Ribeiro^{*} and A. Klümper[†]

^{*} Departamento de Física, Universidade Federal de São Carlos
São Carlos, SP 13565-905, Brazil

[†] Theoretische Physik, Bergische Universität Wuppertal,
42097 Wuppertal, Germany

Abstract

We study the correlation functions of $SU(n)$, $n > 2$, invariant spin chains in the thermodynamic limit. We formulate a consistent framework for the computation of short-range correlation functions via functional equations which hold even at finite temperature. We give the explicit solution for two- and three-site correlations for the $SU(3)$ case at zero temperature. The correlators do not seem to be of factorizable form. From the two-sites result we see that the correlation functions are given in terms of Hurwitz' zeta function, which differs from the $SU(2)$ case where the correlations are expressed in terms of Riemann's zeta function of odd arguments.

^{*}E-mail: pavan@df.ufscar.br

[†]E-mail: kluemper@uni-wuppertal.de

1 Introduction

The study of correlation functions of integrable quantum spin chains has a very long history [1, 2]. There exist many results for the case of the $SU(2)$ spin-1/2 chain [3, 4, 5, 6, 7, 8, 9, 10, 11, 12, 13, 14] and its higher-spin realizations [15, 16, 17, 18, 19, 20, 21].

The correlation functions for the $SU(2)$ spin-1/2 case were realized to be given in terms of Riemann's zeta function of odd arguments [8]. Later higher-spin cases were studied and explicit results were obtained where also zeta function values for even arguments appeared [20, 21]. These results were obtained from solutions of functional equations for suitably defined correlation functions. The derivation of the functional equations is based on the Yang-Baxter equation, and crossing symmetry (valid in the $SU(2)$ case) for the R -matrix, see [14] for the finite temperature case.

Nevertheless, one still lacks a better understanding of the correlation properties of models based on high rank algebras. In the $SU(n)$ case for $n > 2$ [22, 23], there is no result for correlation functions and this stayed as a longstanding problem for decades. In this paper, we devise a framework to tackle the problem of computing the short-range correlations of the integrable $SU(n)$ spin chains. We also provide explicit solutions for the first correlation functions for the $SU(3)$ case, where already for the two-site case the solution is given in terms of Hurwitz' zeta function (generalized zeta function). Besides that, we have indications of the absence of factorization of the correlations in terms of two-point correlations.

This paper is organized as follows. In section 2, we introduce the integrable Hamiltonians and their associated integrable structure. In section 3, we introduce the density operator containing all correlation data as well as a generalized density operator. In contrast to the standard density operator, the generalized density operator allows for the derivation of discrete functional equations. This and the

analyticity properties of the generalized density operator are presented in section 4. In section 5, we exemplify our approach for the case of $SU(3)$ spin chains and we present the zero temperature solution for two- and three-site correlation functions for which the use of a mixed density operator proves to be sufficient. In section 6, we present some evidence for the absence of factorization of the correlations in terms of two-point correlations. Finally, our conclusions are given in section 7. Additional details are given in the appendices.

2 The integrable model

The Hamiltonian of the integrable $SU(n)$ spin chain is given by [22, 23],

$$H^{(n)} = \sum_{j=1}^L P_{j,j+1}, \quad (1)$$

where $P_{j,j+1}$ is the permutation operator and L is the number of sites. The Hilbert space is $V^{\otimes L}$ with local space $V = \mathbb{C}^n$.

For instance, in the case of $SU(3)$ spin chains the Hamiltonian can be written in terms of spin-1 matrices as follows,

$$H^{(3)} = \sum_{j=1}^L [\vec{S}_j \cdot \vec{S}_{j+1} + (\vec{S}_j \cdot \vec{S}_{j+1})^2]. \quad (2)$$

The integrable Hamiltonian (1) is obtained as the logarithmic derivative of the row-to-row transfer matrix

$$T^{(n)}(\lambda) = \text{Tr}_{\mathcal{A}} [R_{\mathcal{A}L}^{(n,n)}(\lambda) \dots R_{\mathcal{A}1}^{(n,n)}(\lambda)], \quad (3)$$

where the R -matrix $R_{ab}^{(n,n)}(\lambda) = P_{ab} \check{R}_{ab}^{(n,n)}(\lambda)$ acts non-trivially on the indicated space $V_a \otimes V_b$ of the (long) tensor product where V_a and V_b are copies of the local space V . The operation of $R_{ab}^{(n,n)}$ is co-variant under $SU(n)$ acting by the product of two fundamental representations $[n]$. The representation $[n]$ is the irreducible

representation of dimension n denoted by a single box in the Young-Tableaux notation. Later in applications we will associate spectral parameters λ, μ with the two local vector spaces the R -matrix acts on and the difference $\lambda - \mu$ will enter as argument. The rational solution of the Yang-Baxter equation can be written and depicted as,

$$\check{R}_{12}^{(n,n)}(\lambda - \mu) = I_{12} + (\lambda - \mu)P_{12} = \begin{array}{c} \lambda \\ | \\ \hline \uparrow \mu \end{array} = \begin{array}{c} \cup \\ \cap \end{array} + (\lambda - \mu) \begin{array}{c} | \\ | \\ \hline | \end{array}, \quad (4)$$

where P_{12} is the standard permutation operator such that $P_{12} = \sum_{i,j,k,l=1}^n P_{ik}^{jl} \hat{e}_{ij}^{(1)} \otimes \hat{e}_{kl}^{(2)}$ with $P_{ik}^{jl} = \delta_{il} \delta_{jk}$ and where $\hat{e}_{ij}^{(a)} \in C_a^n$ are the standard $n \times n$ Weyl matrices acting in the a -space. Likewise, the matrix elements of the identity matrix are given as $I_{ik}^{jl} = \delta_{ij} \delta_{kl}$.

Let us motivate the graphical depiction of algebraic quantities. In the main body of this paper we are going to study correlation functions which occur as ratios of certain (large) sums. The denominator will be the partition function of a certain classical vertex model on a square lattice or a minor modification thereof and the numerator will be a similar partition function of a slightly modified geometry with a few bonds cut and specifically chosen spin values at the open ends. The general rule for turning a graph into a number is like we are used from Feynman diagrams. We place spin variables on closed bonds, we evaluate all local objects for the given spin configuration and multiply these results, which are then summed over for all allowed spin configurations. In particular, a trace over a product of (transfer) matrices naturally turns into a (huge) sum over products of local objects. Very generally, graphs encode contractions of products of tensors.

Note that $R^{(n,n)}$ acts on $[n] \otimes [n]$, understood as $SU(n)$ module, which is graphically indicated by arrows from left to right and from bottom to top. By use of the isomorphism of $\text{End}(W)$ and $W^* \otimes W$ for any linear space W and its dual

W^* we may alternatively view $R^{(n,n)}$ as a vector in the tensor space $[\bar{n}] \otimes [\bar{n}] \otimes [n] \otimes [n]$, i.e. a multilinear map of the type $[n] \times [n] \times [\bar{n}] \times [\bar{n}] \rightarrow \mathbb{C}$.

In order to further illustrate, we show how to read the matrix elements of the R -matrix (4) and the other operators in the graphical notation as follows,

$$[\check{R}^{(n,n)}(\lambda - \mu)]_{ik}^{jl} = I_{ik}^{jl} + (\lambda - \mu)P_{ik}^{jl} = i \begin{array}{c} j \\ \lambda \downarrow \\ \uparrow \mu \\ k \end{array} l = i \begin{array}{c} j \\ \cup \\ k \end{array} l + (\lambda - \mu) i \begin{array}{c} j \\ \downarrow \\ k \end{array} l. \quad (5)$$

The R -matrix with mixed representations of the fundamental $[n]$ and anti-fundamental $[\bar{n}]$ representation of the $SU(n)$ can be written as follows,

$$\check{R}_{12}^{(n,\bar{n})}(\lambda - \mu) = E_{12} + (\lambda - \mu)P_{12} = \begin{array}{c} \cup \\ \downarrow \end{array} + (\lambda - \mu) \begin{array}{c} \downarrow \\ \downarrow \end{array}. \quad (6)$$

where E_{12} is the standard Temperley-Lieb operator such that $E_{ik}^{jl} = \delta_{ik}\delta_{jl}$ and the anti-fundamental representation is the other n dimensional irreducible representation denoted as a column of $n - 1$ boxes in the Young-Tableaux notation. Note the reversed direction of the arrow on the vertical line. For rational models, the remaining combinations can be expressed in terms of the previous one such that $\check{R}^{(\bar{n},n)}(\lambda) = \check{R}^{(n,\bar{n})}(\lambda)$ and $\check{R}^{(\bar{n},\bar{n})}(\lambda) = \check{R}^{(n,n)}(\lambda)$ as linear operators on $V \otimes V$. Note that co-variance with respect to $SU(n)$ is guaranteed, i.e. $g \otimes g^*$ and $g^* \otimes g$ for any $g \in SU(n)$ commute with $\check{R}^{(\bar{n},n)}$ and of course with $\check{R}^{(n,\bar{n})}(\lambda)$.

With a grain of salt, these four R -matrices are solution to the Yang-Baxter equation

$$\check{R}_{12}^{(r_1,r_2)}(\lambda - \mu) \check{R}_{23}^{(r_1,r_3)}(\lambda - \nu) \check{R}_{12}^{(r_2,r_3)}(\mu - \nu) = \check{R}_{23}^{(r_2,r_3)}(\mu - \nu) \check{R}_{12}^{(r_1,r_3)}(\lambda - \nu) \check{R}_{23}^{(r_1,r_2)}(\lambda - \mu), \quad (7)$$

where $r_i \in \{n, \bar{n}\}$ for $i = 1, 2, 3$. For having (7) literally for all combinations of r_1, r_2, r_3 we would have to introduce a shift by n in the argument of for instance

$\check{R}^{(n,\bar{n})}$ wherever it appears. However, we keep the definitions of the R -matrices as given above and have (7) for all r_1, r_2, r_3 except for n, \bar{n}, n and \bar{n}, n, \bar{n} . In order to simplify our notation it is convenient to list these equations in a group of six standard equations as above (7) and a group of two special ones which have shifted arguments in the intertwining matrix (see Figure 1). We explicitly write one of the special Yang-Baxter equations,

$$\check{R}_{12}^{(n,\bar{n})}(\lambda-\mu+n)\check{R}_{23}^{(n,n)}(\lambda-\nu)\check{R}_{12}^{(\bar{n},n)}(\mu-\nu) = \check{R}_{23}^{(\bar{n},n)}(\mu-\nu)\check{R}_{12}^{(n,n)}(\lambda-\nu)\check{R}_{23}^{(n,\bar{n})}(\lambda-\mu+n), \quad (8)$$

and the other one is obtained by exchanging the representations $[n]$ and $[\bar{n}]$. It is worth to note that in our graphical notation, e.g in Figure 1, the lines upwards and to the right are associated to the fundamental representation $[n]$ and conversely the lines downwards and to the left are associated to the anti-fundamental representation $[\bar{n}]$.

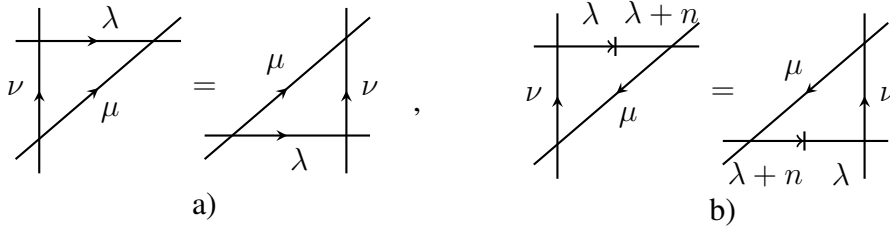


Figure 1: Graphical illustration of the Yang-Baxter equation (where vertices from lower left to upper right correspond to R -matrices in (7) and (8) from right to left): a) the standard Yang-Baxter equation (7) for the fundamental representation $r_1 = r_2 = r_3 = [n]$ (the 5 remaining standard equations are obtained from a) by rotation); b) the special Yang-Baxter equation (8), where the shift in the argument of the R -matrix can be conveniently seen as a discontinuity of the spectral parameter along that line.

The fundamental R -matrix has important properties,

$$\check{R}_{12}^{(n,n)}(0) = I, \quad \text{initial condition,} \quad (9)$$

$$\check{R}_{12}^{(n,n)}(\lambda - \mu) \check{R}_{21}^{(n,n)}(\mu - \lambda) = (1 - (\lambda - \mu)^2) I, \quad \text{standard unitarity,} \quad (10)$$

where again I is the $n^2 \times n^2$ identity matrix. These relations hold literally also for $\check{R}^{(\bar{n}, \bar{n})}$. However, differently from the $SU(2)$ case, the $SU(n)$ case for $n > 2$ does not have crossing symmetry, which makes this model special in the realm of integrable models. This is because for $n > 2$ the conjugate of the representation $[n]$, namely $[\bar{n}]$, is inequivalent to $[n]$.

In order to circumvent the difficulties which arise from the fact that the model lacks the crossing symmetry, one has to add a few more ingredients to formulate a consistent framework for the computation of correlation functions. The crucial observation is that one has to conveniently and largely on the same footing work with the fundamental $[n]$ and anti-fundamental representation $[\bar{n}]$ of the $SU(n)$. This is possible since as presented before, the Yang-Baxter equation accommodates different representations in each vector space. Besides that, the above R -matrices with mixed representations also have symmetry properties, which we call special unitarity (see Figure 2b),

$$\check{R}_{12}^{(n, \bar{n})}(\lambda - \mu + n) \check{R}_{21}^{(\bar{n}, n)}(\mu - \lambda) = (\mu - \lambda)(\lambda - \mu + n) I, \quad (11)$$

$$\check{R}_{12}^{(\bar{n}, n)}(\lambda - \mu) \check{R}_{21}^{(n, \bar{n})}(\mu - \lambda + n) = (\lambda - \mu)(\mu - \lambda + n) I. \quad (12)$$

Finally, in order to exploit the full $SU(n)$ symmetry we introduce relations of suitable products of n many R -matrices with the completely antisymmetric state in $V^{\otimes n}$, i.e. the totally antisymmetric tensor ϵ . For instance, in the $SU(3)$ case

$$\begin{array}{cc}
\begin{array}{c} \text{Diagram a: A crossing of two lines with spectral parameters } \mu \text{ and } \lambda. \end{array} & = (1 - (\lambda - \mu)^2) \begin{array}{c} \text{Diagram b: A crossing of two lines with spectral parameters } \mu \text{ and } \lambda + n. \end{array} \\
\text{a)} & \text{b)}
\end{array}$$

Figure 2: Graphical illustration of the unitarity relations (two more are obtained by 180° rotations): a) the standard unitarity (10); b) the special unitarity (11). Again we consider the spectral parameter to be discontinuous in order to describe the shift in the R -matrix, i.e. the spectral parameter value is $\lambda + n$ in the bottom part and λ in the top part of the graph.

these relations read,

$$\begin{array}{c} \lambda \\ \leftarrow \\ \lambda + 1 \\ \leftarrow \\ \lambda + 2 \\ \leftarrow \\ \mu \end{array} = (\lambda + 2 - \mu)(1 - (\lambda - \mu)^2) \begin{array}{c} \lambda \\ \leftarrow \\ \lambda + 1 \\ \leftarrow \\ \lambda + 2 \\ \leftarrow \\ \mu \end{array}, \quad (13)$$

and

$$\begin{array}{c} \lambda \\ \leftarrow \\ \lambda + 1 \\ \leftarrow \\ \lambda + 2 \\ \leftarrow \\ \mu \end{array} = (\mu - \lambda)(1 - (\lambda + 2 - \mu)^2) \begin{array}{c} \lambda \\ \leftarrow \\ \lambda + 1 \\ \leftarrow \\ \lambda + 2 \\ \leftarrow \\ \mu \end{array}, \quad (14)$$

and the depicted objects are

$$\begin{array}{c} k \\ \bullet \\ j \\ \bullet \\ i \\ \bullet \end{array} = \epsilon_{ijk}, \quad \begin{array}{c} j \\ \bullet \\ \uparrow \\ \bullet \\ i \end{array} = \delta_{ij} \quad (15)$$

the fully anti-symmetric tensor (Levi-Civita tensor) and the Kronecker delta. Besides that, a number of simple identities among the previous objects are used throughout this work, e.g. tensor products and contractions

$$\begin{aligned}
 & \text{Diagram 1: A square with three horizontal lines. The top line has a dot labeled k, the middle line has a dot labeled j, and the bottom line has a dot labeled i. The left and right sides are connected by vertical lines.} = \epsilon_{ijk} \epsilon^{ijk} = 6, \\
 & \text{Diagram 2: A circle with a dot labeled i at the top.} = \delta_{ii} = 3 \quad (16) \\
 & \text{Diagram 3: A vertical line with a dot labeled l at the top, a dot labeled j on the left, a dot labeled k on the right, and a dot labeled i at the bottom. The left and right sides are connected by a vertical line.} = 2 \text{Diagram 4: A vertical line with a dot labeled l at the top and a dot labeled i at the bottom.} = \epsilon_{ijk} \epsilon^{jkl} = 2\delta_{il}, \\
 & \text{Diagram 5: A diagram with two vertical lines. The left line has a dot labeled l at the top and a dot labeled i at the bottom. The right line has a dot labeled m at the top and a dot labeled j at the bottom. They are connected by a horizontal line with a dot labeled k in the middle.} = \text{Diagram 6: Two vertical lines, each with a dot labeled l at the top and a dot labeled i at the bottom. They are connected by a horizontal line with a dot labeled m in the middle.} - \text{Diagram 7: Two vertical lines, each with a dot labeled l at the top and a dot labeled i at the bottom. They are connected by a horizontal line with a dot labeled m in the middle. The lines cross each other.} = \epsilon_{ijk} \epsilon^{klm} = \delta_{il} \delta_{jm} - \delta_{im} \delta_{jl} \quad (17)
 \end{aligned}$$

3 Density matrices

The framework for calculating thermal correlation functions of integrable Hamiltonians was introduced in [24] and has been applied to the case of integrable $SU(2)$ spin chains several times, see e.g. [19, 20, 21]. This approach makes use of the usual inhomogeneous reduced density operator, see Figure 3a, in the thermodynamic limit $L \rightarrow \infty$, however with finite Trotter number N [24]. This formulation can be naturally extended to the case of $SU(n)$ spin chains. As the infinitely many column-to-column transfer matrices on the left (right) project onto the leading eigenstate $\langle \Phi_L |$ ($|\Phi_R\rangle$) we obtain the compact form

$$D_m(\lambda_1, \dots, \lambda_m) = \frac{\langle \Phi_L | \mathcal{T}_1^{(n)}(\lambda_1) \cdots \mathcal{T}_m^{(n)}(\lambda_m) | \Phi_R \rangle}{\Lambda_0^{(n)}(\lambda_1) \cdots \Lambda_0^{(n)}(\lambda_m)}, \quad (18)$$

where $\mathcal{T}_j^{(n)}(x)$ is the usual j -th monodromy matrix $\mathcal{T}_j^{(n)}(x) = R_{j,N}^{(n,n)}(x - u_N) \cdots R_{j,2}^{(n,n)}(x - u_2) R_{j,1}^{(n,n)}(x - u_1)$ associated to the quantum transfer matrix for the $SU(n)$ quantum spin chains $t_j^{QTM}(x) = \text{Tr}[\mathcal{T}_j^{(n)}(x)]$, Φ_L and Φ_R represent the left and right leading eigenstates of the quantum transfer matrix and $\Lambda_0^{(n)}(x)$ is the leading eigenvalue. For instance, the matrix element $D_{m11\dots 1}^{11\dots 1} = \text{Tr} \left[\hat{e}_{11}^{(1)} \hat{e}_{11}^{(2)} \cdots \hat{e}_{11}^{(m)} D_m \right]$

(which in Figure 3 corresponds to assign 1 to all the indices sitting at the black dots) is the standard emptiness formation probability $P_m(\lambda_1, \dots, \lambda_m)$ [1, 25].

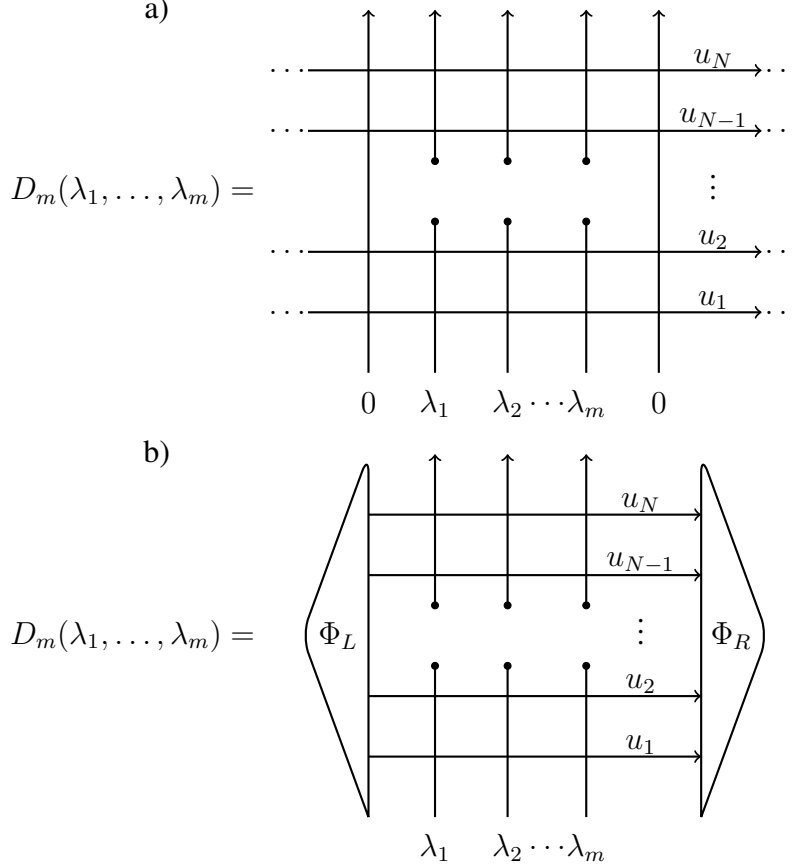


Figure 3: Graphical illustration of the un-normalized density operator $D_m(\lambda_1, \dots, \lambda_m)$: a) an infinite cylinder with N infinitely long horizontal lines carrying spectral parameters u_j and m open bonds associated to the spectral parameters $\lambda_1, \dots, \lambda_m$; b) the infinitely many column-to-column transfer matrices to the left and to the right are replaced by the boundary states they project onto.

The physically interesting result is typically obtained from the above reduced density operator (18) by taking the homogeneous limit $\lambda_j \rightarrow 0$ and the Trotter limit $N \rightarrow \infty$. However, we take advantage of the dependence on arbitrary

$\lambda \in \mathbb{C}$. For the density operator of the $SU(2)$ case a set of discrete functional equations can be derived by use of the usual integrability structure plus the crossing symmetry [14]. This and transparent analyticity properties allow for the complete determination of the reduced density operator at finite temperature and for an alternative proof of factorization of the correlation functions in terms of sums over products of nearest-neighbor correlators.

Unfortunately, for the case of $SU(n)$ spin chains with $n > 2$ we do not have crossing symmetry and hence adopting the line of reasoning of the $SU(2)$ case does not result in a closed set of functional equations for D_m . However, we can derive an analogous set of discrete functional equations provided we consider a slightly more general density operator we denote by $\mathbb{D}_m(\lambda_1, \dots, \lambda_m)$. Like the usual density operator, the generalized density operator \mathbb{D}_m is defined on a horizontal infinite cylinder with N horizontal lines, carrying spectral parameters u_j , however with additional semi-infinite rows as depicted in Figure 4a. Alternatively, this generalized correlator can be written with boundary states where now $\tilde{\Phi}_L$ is the leading eigenstate of the modified quantum transfer matrix acting on a tensor product of $N + m \cdot n$ copies of V (see Figure 4b). The monodromy matrix is given by $\tilde{\mathcal{T}}_j^{(n)}(x) = \mathcal{T}_j^{(n)}(x) \cdot \prod_{\alpha=1}^m \prod_{\beta=1}^n R_{j, N+(\alpha-1)n+\beta}^{(n, \bar{n})}(x - (\lambda_\alpha + \beta - 1))$.

Besides the correlations contained in D_m , the generalized density operator \mathbb{D}_m also contains other correlation functions, like those contained in variants of D_m with just anti-fundamental representations or any mixture of fundamental and anti-fundamental representations in the spaces indexed by 1 to m .

Note that D_m may be viewed as a vector in the tensor space $[\bar{n}]^{\otimes m} \otimes [n]^{\otimes m}$, i.e. a multilinear map $[n]^m \times [\bar{n}]^m \rightarrow \mathbb{C}$, and likewise \mathbb{D}_m is a vector in the tensor space $[\bar{n}]^{\otimes mn}$, i.e. a multilinear map $[n]^{mn} \rightarrow \mathbb{C}$.

We have to show that

- the generalized density operator \mathbb{D}_m contains the physically interesting cor-

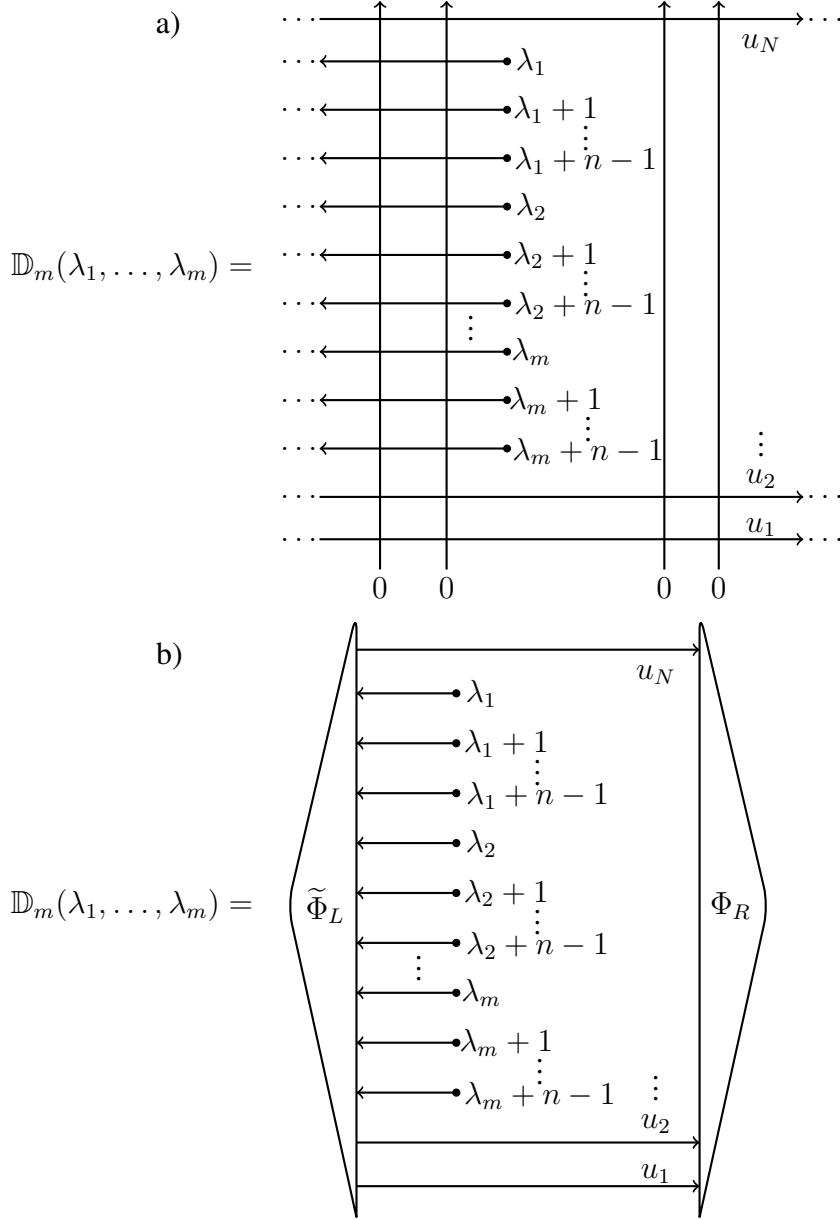


Figure 4: Graphical illustration of the un-normalized generalized density operator $\mathbb{D}_m(\lambda_1, \dots, \lambda_m)$: a) the infinite cylinder with N infinitely long horizontal lines carrying spectral parameters u_j and m bunches of n semi-infinite lines with spectral parameters $\{\lambda_j, \lambda_j + 1, \dots, \lambda_j + n - 1\}$ for $j = 1, \dots, m$; b) the infinitely many column-to-column transfer matrices to the left and to the right are replaced by the boundary states they project onto.

relations (and more),

- it admits a closed set of functional equations,
- it has controlled analyticity properties (which are not obvious from the definition).

Before turning to the proofs we like to mention the normalization of the generalized density operator. For this we take the action of $\mathbb{D}_m(\lambda_1, \dots, \lambda_m)$ on m completely antisymmetric states (the $SU(n)$ singlets) in each bunch of n basis states. We like to mention the useful reduction property of \mathbb{D}_m applied to just k antisymmetric states resulting into a density matrix \mathbb{D}_{m-k} , see Appendix A.

Next we turn to the embedding of D_m in \mathbb{D}_m . For this we apply anti-symmetrizations to the lower (upper) $n - 1$ lines of a bunch of n lines in \mathbb{D}_m resulting in a line carrying the conjugate representation. For the $SU(3)$ case we have:

$$\begin{array}{c} \uparrow \uparrow \\ \leftarrow \begin{array}{|c|} \hline \lambda \\ \hline \lambda + 1 \\ \hline \lambda + 2 \end{array} \rightarrow \\ \leftarrow \quad \quad \quad \rightarrow \\ \leftarrow \quad \quad \quad \rightarrow \end{array} = \begin{array}{c} \uparrow \uparrow \\ \leftarrow \begin{array}{|c|} \hline \lambda \\ \hline \lambda \\ \hline \end{array} \rightarrow \\ \leftarrow \quad \quad \quad \rightarrow \end{array}, \quad (19)$$

$$\begin{array}{c} \uparrow \uparrow \\ \leftarrow \begin{array}{|c|} \hline \lambda \\ \hline \lambda + 1 \\ \hline \lambda + 2 \end{array} \rightarrow \\ \leftarrow \quad \quad \quad \rightarrow \\ \leftarrow \quad \quad \quad \rightarrow \end{array} = \begin{array}{c} \uparrow \uparrow \\ \leftarrow \begin{array}{|c|} \hline \lambda - 1 \\ \hline \lambda + 2 \\ \hline \end{array} \rightarrow \\ \leftarrow \quad \quad \quad \rightarrow \end{array}. \quad (20)$$

Let us consider the anti-symmetrization of the lower $n - 1$ lines. In Figure 5 we depict the simplest case of two-point ($m = 2$) correlations for $SU(3)$. First, the antisymmetrizers are carried to the very left by virtue of (19), see Figure 5 a) and b). We modify the lattice at the far left by bending the upper horizontal line with arrow pointing to the left upwards and bending the lower horizontal line with

arrow pointing to the right downwards, finally connecting the two ends (carrying the same spectral parameter) by exploiting the periodic boundary condition in vertical direction, Figure 5 c). This manipulation of the far left boundary may introduce a factor which however is independent of the spins on the open bonds inside the lattice. Finally, we use the Yang-Baxter equation and unitarity to move the closed loops at the far left as simple vertical lines to the center of the lattice, Figure 5 d) and e). The resulting object is equal to the density operator $D_2(\lambda_1, \lambda_2)$ under the action of two R -matrices.

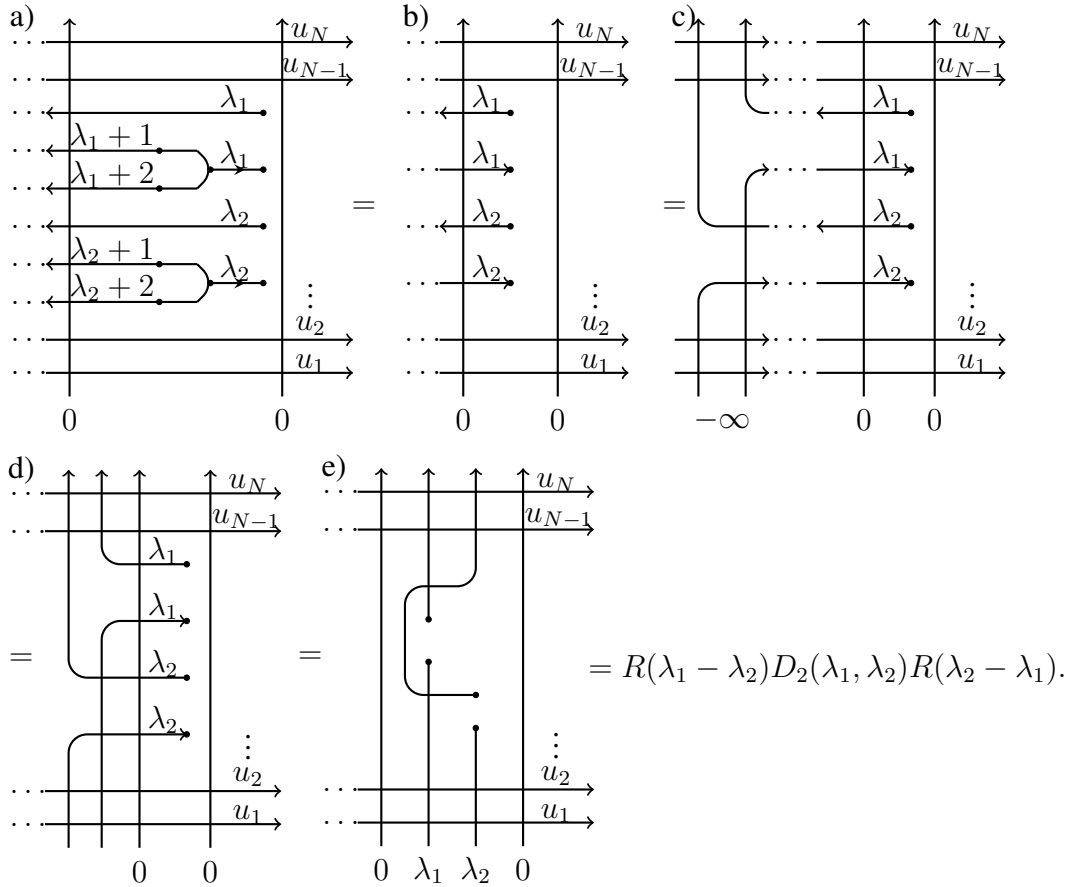


Figure 5: Graphical illustration of the reduction of the generalized density operator $\mathbb{D}_2(\lambda_1, \lambda_2)$ to the density operator $D_2(\lambda_1, \lambda_2)$ for $SU(3)$.

Quite generally, by the above described procedure of anti-symmetrization of the lower $n - 1$ lines of each bunch of n lines we have the reduction of the operator $\mathbb{D}_m(\lambda_1, \dots, \lambda_m)$ to the usual density operator $D_m(\lambda_1, \dots, \lambda_m)$ with additional action of $m(m - 1)$ R -matrices.

Just as a short remark we want to point out that the procedure of anti-symmetrization of the *upper* $n - 1$ lines of a bunch of n lines and subsequent use of Yang-Baxter and (special) unitarity leads to a vertical line with conjugate representation of $SU(n)$ and carrying the spectral parameter $\lambda + n - 1$.

It is worth reminding that the physically interesting object we want to compute is precisely the full density operator D_m . However, in order to formulate consistent functional equations we have to work in the more general setting of \mathbb{D}_m and at the end of the calculation to project onto the physically relevant subspace. The derivation of functional equations and analyticity properties for \mathbb{D}_m is the subject of the next section.

4 Discrete functional equations and analyticity

In order to derive closed functional equations for the correlators of the $SU(n)$ quantum spin chain, we explore the consequences of setting the value of for instance λ_1 equal to one of the spectral parameters u_i on the horizontal lines. We illustrate a sequence of manipulations in Figure 6 for the case $m = 2$ of $SU(3)$.

Having $\lambda_1 = u_i$ allows us to connect the left going semi-infinite line carrying λ_1 with the right-going line carrying u_i , Figure 6a, and to use the unitarity property (10) for moving the link towards the right, Figure 6 b) and c). Note that operation a) may change the partition function by some factor which however is independent of the spins on the interior open bonds. Next, we use special unitarity (11) to move the line around and back to the left, Figure 6 d) and e).

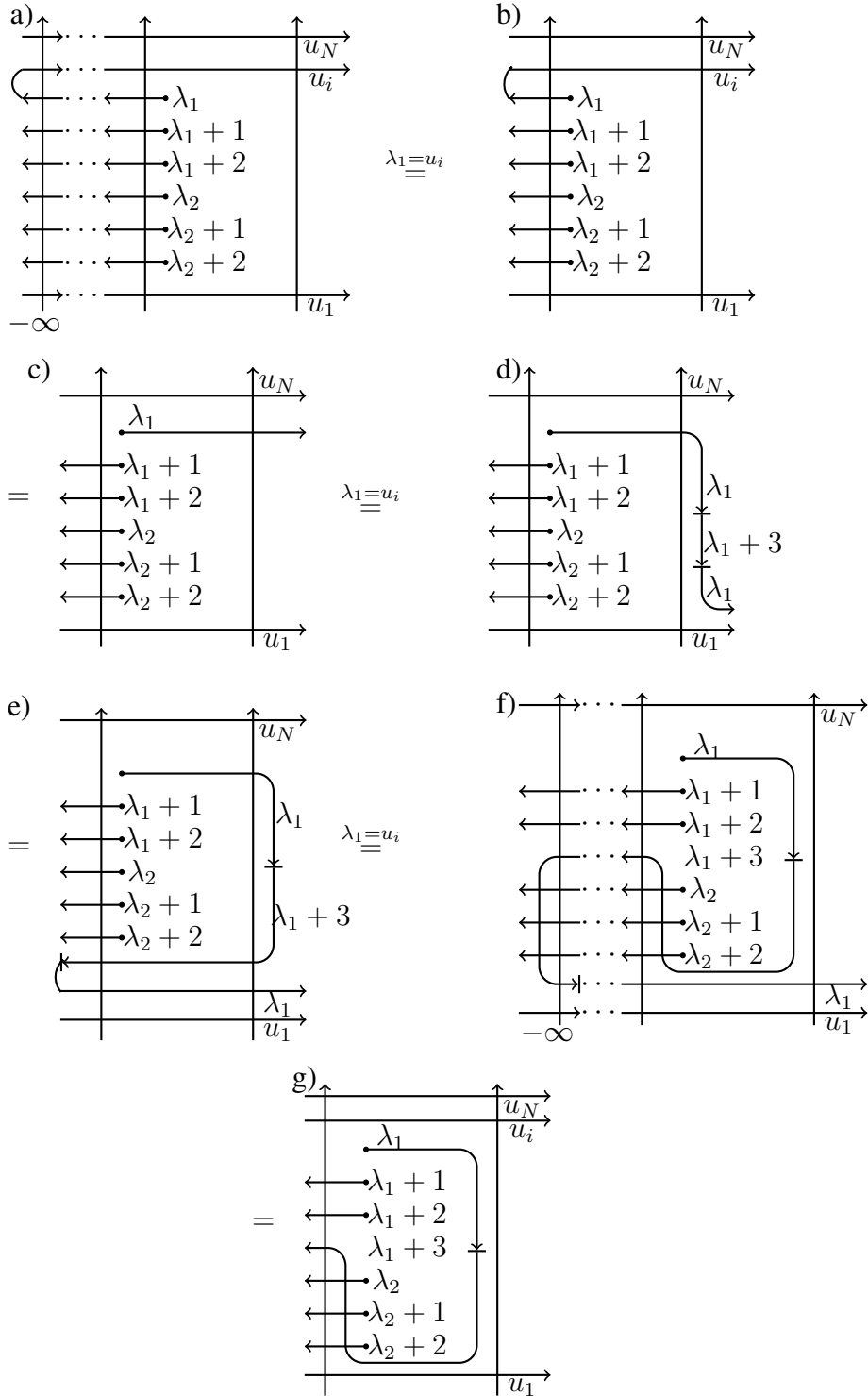


Figure 6: Outline of the derivation of the functional equation for the two-sites ($m = 2$) generalized density operator for the $SU(3)$ case.

Then we use standard unitarity and widen the narrow loop as shown in Figure 6 f). This introduces the action of additional R -matrices at the open ends in the middle part of the lattice and at the far left, Figure 6 f). The boundary part at $-\infty$ is dropped, the horizontal line carrying λ_1 is moved by use of periodic boundary condition in vertical direction as u_i line upwards. Finally we obtain the original density operator with the spectral parameter λ_1 shifted by 1 with the action of R -matrices upon it, Figure 6 g).

In summary, for arbitrary m and $SU(n)$ we derive a functional equation for the generalized density operator $\mathbb{D}_m(\lambda_1, \dots, \lambda_m)$ given by,

$$\mathbb{A}_m(\lambda_1, \dots, \lambda_m)[\mathbb{D}_m(\lambda_1 + 1, \lambda_2, \dots, \lambda_m)] = \mathbb{D}_m(\lambda_1, \lambda_2, \dots, \lambda_m), \quad \lambda_1 = u_i, \quad (21)$$

where the linear $\mathbb{A}_m(\lambda_1, \dots, \lambda_m)$ operator is a product of $(m-1)n$ R -matrices given as

$$\begin{aligned} \mathbb{A}_m(\lambda_1, \dots, \lambda_m)_{i_1 \dots i_{nm}}^{i_1 \dots i_{nm}} &:= \prod_{k=1}^{m-1} \prod_{j=1+(k-1)n}^{kn} \check{R}^{(n,n)}(\lambda_1 - \lambda_{m-k+1} + j)_{\alpha_j, \bar{i}_j}^{i_j, \alpha_{j-1}} \\ &\times \delta_{\alpha_0}^{i_{nm}} \delta_{i_{n(m-1)+1}}^{\alpha_{n(m-1)+1}} \delta_{i_{n(m-1)+2}}^{i_{n(m-1)+1}} \dots \delta_{i_{nm}}^{i_{nm-1}}, \end{aligned} \quad (22)$$

where we assume summation over repeated indices α_j . The action of $\mathbb{A}_2(\lambda_1, \lambda_2)$ for arbitrary $SU(n)$ is illustrated in Figure 7.

Next we turn to the analytical properties of $\mathbb{D}_m(\lambda_1, \dots, \lambda_m)$. By definition, an infinite number of vertices carrying the parameters λ_j enter which may result in an uncontrolled analytical dependence. Here we are going to show that fortunately this is not so.

In order to represent the density operator in a way that the analyticity properties become transparent, we attach at the far left boundary the operator defined graphically on the left hand side of Figure 8. This operator can be moved inside the lattice by use of the 180° rotated version of (13-14), as well as unitarity and special unitarity, see Figure 8.

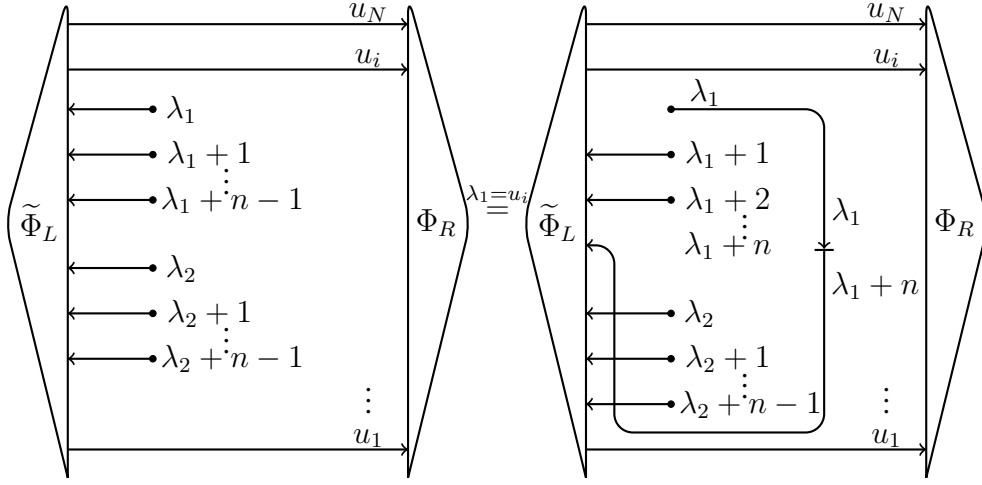


Figure 7: Graphical illustration of the functional equations for two-sites ($m = 2$) for the generalized density operator $\mathbb{D}_2(\lambda_1, \lambda_2)$ valid for $\lambda_1 = u_i$. Note that the spectral parameter on the manipulated line is λ_1 on the left hand side, and $\lambda_1 + n$ on the right hand side.

This manipulation makes the analytical structure of the generalized density operator $\mathbb{D}_m(\lambda_1, \dots, \lambda_m)$ clear. For the $SU(3)$ case illustrated in Figure 8 the numerator of the (unnormalized) matrix elements must be a multivariate polynomial of degree $2N$ in the variables λ_j times an N independent number of linear factors of the type $\lambda_i - \lambda_j + \text{const.}$ Therefore, the matrix elements of the generalized density operator after normalization are of the kind,

$$\frac{P(\lambda_1, \dots, \lambda_m)}{\prod_{i=1}^m \Lambda_0^{(3)}(\lambda_i) \Lambda_0^{(\bar{3})}(\lambda_i + 2) \cdot \prod_{i < j} \Phi(\lambda_i - \lambda_j)}, \quad (23)$$

where $P(\lambda_1, \dots, \lambda_m)$ is a multivariate polynomial of degree up to $2N + 6(m - 1)m/2$ in each variable, $\Phi(\delta) := (4 - \delta^2)(1 - \delta^2)^2$ from the intersection of three semi-infinite lines with two vertical lines and $\Lambda_0^{(3)}(\lambda)$ is the leading eigenvalue of the quantum transfer matrix with fundamental representation in the auxiliary space and $\Lambda_0^{(\bar{3})}(\lambda)$ is the leading eigenvalue of the quantum transfer matrix with anti-fundamental representation in the auxiliary space. The normalization in the

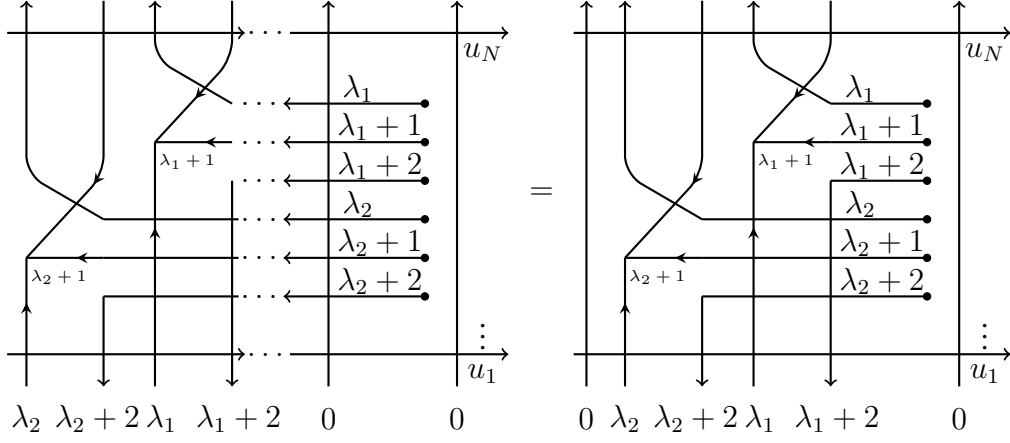


Figure 8: The generalized density operator $\mathbb{D}_m(\lambda_1, \dots, \lambda_m)$ for the case $SU(3)$ and $m = 2$, i.e. two bunches of semi-infinite lines. The semi-infinite lines can be rearranged without changing the correlations in the form of two vertical lines with spectral parameters λ_i and $\lambda_i + 2$, however with different arrow directions resp. representations.

denominator is obtained by use of (13-14) to move the lower anti-symmetrizer to the left, which generates the $\Phi(\delta)$ function. Finally, by use of properties (16-17) we obtain two decoupled up- and down- going lines with spectral parameters λ_i and $\lambda_i + 2$, which are associated with the corresponding leading eigenvalues.

In the next section, we are going to discuss the solution of the above functional equations for two and three-sites density operators for the case of the $SU(3)$ spin chain.

5 $SU(3)$ spin chain

In order to compute the two ($m = 2$) and three ($m = 3$) sites density operator $\mathbb{D}_m(\lambda_1, \dots, \lambda_m)$ we have to propose a suitable ansatz. This is usually done by choosing a certain number of linearly independent operators (states) as a basis and

working out the resulting equations for the expansion coefficients. However, the number of these operators is determined by the dimension of the singlet subspace of the total space of density operators on m sites referred to as $\dim(m)$, which for the two and three-sites case are 5 and 42, respectively. Although the two-sites case can still be treated, the high number of required independent operators for three-sites makes the problem very hard to treat.

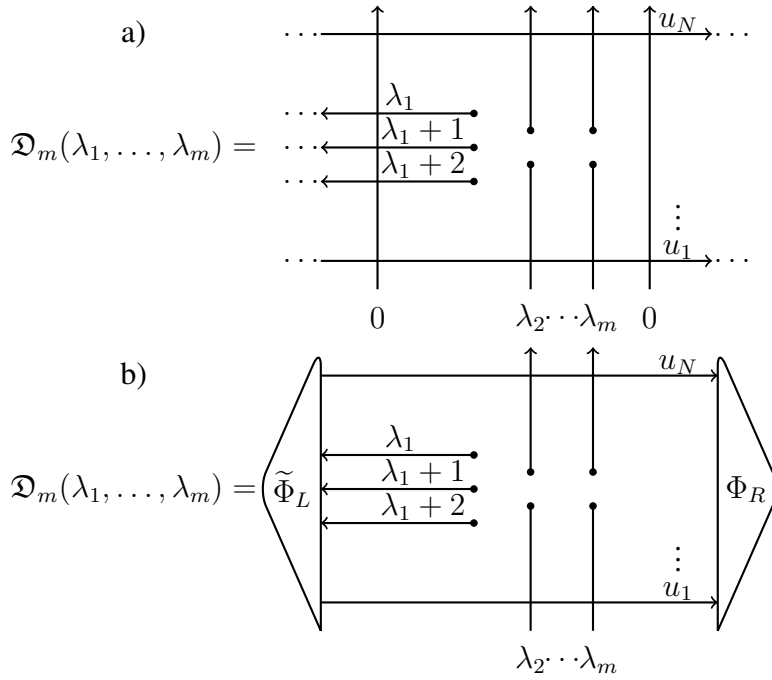


Figure 9: Graphical illustration of the un-normalized mixed density operator $\mathfrak{D}_m(\lambda_1, \dots, \lambda_m)$ for the $SU(3)$ case. a) We have an infinite cylinder with N infinitely long horizontal lines carrying spectral parameters u_j , 1 bunch of three semi-infinite lines carrying spectral parameters $\{\lambda_1, \lambda_1 + 1, \lambda_1 + 2\}$ and $m - 1$ vertically open bonds associated to the spectral parameters $\lambda_2, \dots, \lambda_m$; b) the infinitely many column-to-column transfer matrices to the left and right replaced by the boundary states they project onto.

A crucial observation to turn the three-sites case feasible is to reduce the num-

ber of bunches of semi-infinite horizontal lines to the minimal possible. For the problem at hand we found that this can be done by working with only one bunch of semi-infinite horizontal lines and the remaining $m - 1$ bunches reduced by partial anti-symmetrization to $m - 1$ vertically open bonds resulting in a mixed density operator denoted by $\mathfrak{D}_m(\lambda_1, \dots, \lambda_m)$ (see Figure 9).

This strategy reduces the dimension of the singlet subspace for the two and three-sites case to $\dim(2) = 3$ and $\dim(3) = 11$, respectively. Therefore the density operator can be written as $\mathfrak{D}_m(\lambda_1, \dots, \lambda_m) = \sum_{k=1}^{\dim(m)} \rho_k^{[m]}(\lambda_1, \dots, \lambda_m) P_k^{[m]}$, for conveniently chosen operators $P_k^{[m]}$. In addition, the mixed density operator (Figure 9) has also the advantage of simpler reduction properties, since under partial anti-symmetrization of the semi-infinite lines it is reduced directly to the physical density operator without the action of R -matrices.

The mixed density operator also fulfills a functional equation of the form (21). More specifically the equation satisfied by $\mathfrak{D}_m(\lambda_1, \dots, \lambda_m)$ is shown for the $SU(3)$ case in Figure 10a, which again is derived for $\lambda_1 = u_i$ by use of unitarity, Yang-Baxter and special unitarity condition.

$$\mathfrak{A}_m(\lambda_1, \dots, \lambda_m) [\mathfrak{D}_m(\lambda_1 + 1, \lambda_2, \dots, \lambda_m)] = \mathfrak{D}_m(\lambda_1, \lambda_2, \dots, \lambda_m), \quad \lambda_1 = u_i, \quad (24)$$

where $\mathfrak{A}_m(\lambda_1, \dots, \lambda_m)$ is a linear operator which consists of a product of $2(m-1)$ R -matrices depicted in Figure 10 for the case $SU(3)$, whose expression is given by (see Figure 10b),

$$\begin{aligned} & \mathfrak{A}_m(\lambda_1, \dots, \lambda_m)_{\bar{i}_1 \bar{i}_2 \bar{i}_3 \bar{r}_1 \dots \bar{r}_{m-1} \bar{s}_1 \dots \bar{s}_{m-1}}^{i_1 i_2 i_3 r_1 \dots r_{m-1} s_1 \dots s_{m-1}} = \\ & = [\check{R}^{(3,3)}(\lambda_1 - \lambda_2)]_{\bar{i}_3 r_1}^{\bar{r}_1 \alpha_1} [\check{R}^{(3,3)}(\lambda_1 - \lambda_3)]_{\alpha_1 r_2}^{\bar{r}_2 \alpha_2} \dots [\check{R}^{(3,3)}(\lambda_1 - \lambda_m)]_{\alpha_{m-2} r_{m-1}}^{\bar{r}_{m-1} \alpha_{m-1}} \delta_{\beta_1}^{\alpha_{m-1}} \delta_{i_1}^{\bar{i}_2} \delta_{i_2}^{\bar{i}_3} \\ & \times [\check{R}^{(3,\bar{3})}(\lambda_1 + 3 - \lambda_m)]_{\beta_1 s_{m-1}}^{\bar{s}_{m-1} \beta_2} \dots [\check{R}^{(3,\bar{3})}(\lambda_1 + 3 - \lambda_3)]_{\beta_{m-2} s_2}^{\bar{s}_2 \beta_{m-1}} [\check{R}^{(3,\bar{3})}(\lambda_1 + 3 - \lambda_2)]_{\beta_{m-1} s_1}^{\bar{s}_1 \bar{i}_1}. \end{aligned} \quad (25)$$

As for the generalized density operator, also for the mixed density operator $\mathfrak{D}_m(\lambda_1, \dots, \lambda_m)$ the analytical properties with regard to the dependence on λ_1 are

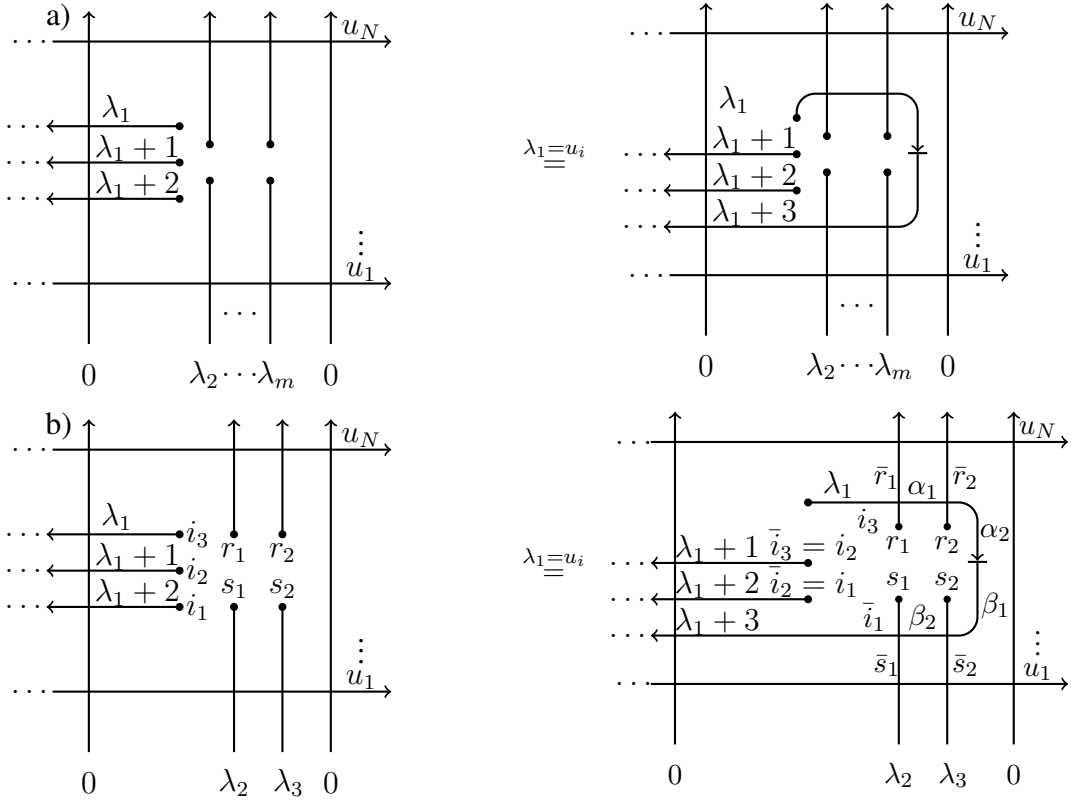


Figure 10: Graphical depiction of the functional equations for the mixed density operator $\mathfrak{D}_m(\lambda_1, \dots, \lambda_m)$ valid for $\lambda_1 = u_i$: for: a) m -sites; b) 3-sites matrix elements.

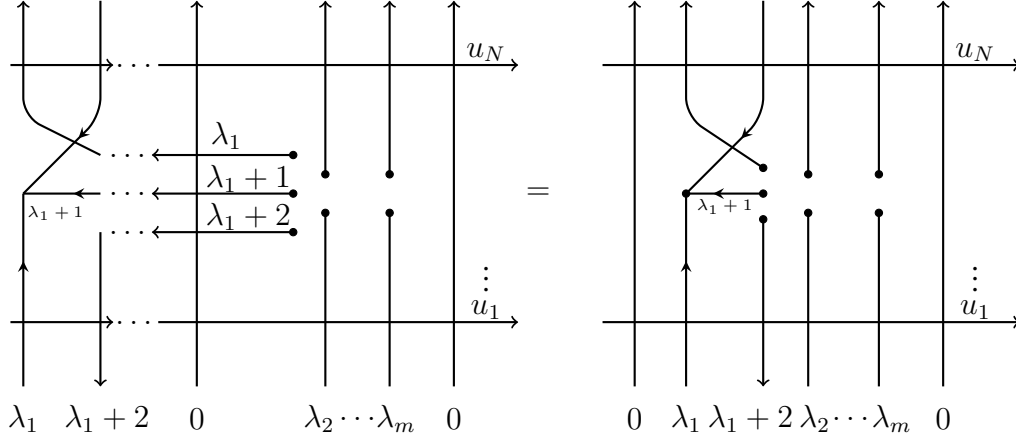


Figure 11: The mixed density operator $\mathfrak{D}_m(\lambda_1, \dots, \lambda_m)$ for the case $SU(3)$ and $m = 3$, i.e. one bunch of semi-infinite horizontal lines and two open vertical lines. The semi-infinite lines can be rearranged without changing the correlations in the form of two vertical lines with spectral parameters λ_1 and $\lambda_1 + 2$, however different arrow directions resp. representations.

not obvious from the definition of the operator. However, by exploiting the properties (13-14) as above, we transform the semi-infinite horizontal lines carrying the spectral parameter λ_1 into two vertical lines, see Figure 11.

This makes the analytical structure of the mixed density operator $\mathfrak{D}_m(\lambda_1, \dots, \lambda_m)$ clear, since for the $SU(3)$ case the numerator of the matrix elements must be a multivariate polynomial of degree $2N$ in the variable λ_1 and of degree N for the remaining λ_i , for $i = 2, 3, \dots, m$,

$$\frac{P(\lambda_1, \dots, \lambda_m)}{\Lambda_0^{(3)}(\lambda_1) \Lambda_0^{(\bar{3})}(\lambda_1 + 2) \prod_{i=2}^m \Lambda_0^{(3)}(\lambda_i)}, \quad (26)$$

where again $\Lambda_0^{(3)}(\lambda)$ is the leading eigenvalue of the quantum transfer matrix with fundamental representation in the auxiliary space and $\Lambda_0^{(\bar{3})}(\lambda)$ is the leading eigenvalue of the quantum transfer matrix with anti-fundamental representation in the auxiliary space.

5.1 Computation of the two-sites density operator

Due to $SU(n)$ symmetry the usual (normalized) two-point density operator for the fundamental-fundamental and also for anti-fundamental–fundamental representations can be written as follows,

$$D_2^{(nn)}(\lambda_1, \lambda_2) = \left(\frac{1}{n^2} - \frac{\alpha_{nn}(\lambda_1, \lambda_2)}{n} \right) I + \alpha_{nn}(\lambda_1, \lambda_2) P, \quad (27)$$

$$D_2^{(\bar{n}n)}(\lambda_1, \lambda_2) = \left(\frac{1}{n^2} - \frac{\alpha_{\bar{n}n}(\lambda_1, \lambda_2)}{n} \right) I + \alpha_{\bar{n}n}(\lambda_1, \lambda_2) E. \quad (28)$$

It is convenient to define some simple two-point correlation functions to work with,

$$\omega_{nn}(\lambda_1, \lambda_2) = \text{Tr}[P D_2^{(nn)}] = \frac{1}{n} + (n^2 - 1)\alpha_{nn}(\lambda_1, \lambda_2), \quad (29)$$

$$\omega_{\bar{n}n}(\lambda_1, \lambda_2) = \text{Tr}[E D_2^{(\bar{n}n)}] = \frac{1}{n} + (n^2 - 1)\alpha_{\bar{n}n}(\lambda_1, \lambda_2). \quad (30)$$

The above correlation functions will be useful in the coming computations.

The operator (27) represents the full density matrix whose non-trivial matrix elements are $D_2^{(nn)ii}(\lambda_1, \lambda_2) = \frac{1}{n^2} + \frac{(n-1)}{n}\alpha_{nn}(\lambda_1, \lambda_2)$, $D_2^{(nn)ji}(\lambda_1, \lambda_2) = \alpha_{nn}(\lambda_1, \lambda_2)$, $D_2^{(nn)ij}(\lambda_1, \lambda_2) = \frac{1}{n^2} - \frac{1}{n}\alpha_{nn}(\lambda_1, \lambda_2)$ for $i, j = 1, \dots, n$, $i \neq j$. Therefore, in order to fully determine the two-sites density operator (27), one only needs to compute $\alpha_{nn}(\lambda_1, \lambda_2)$ or equivalently $\omega_{nn}(\lambda_1, \lambda_2)$ above.

As discussed above, for deriving a closed set of functional equations we have to use the mixed density operator \mathfrak{D}_2 and due to the $SU(3)$ symmetry this operator can be explicitly written as a superposition of 3 linearly independent operators as follows,

$$\mathfrak{D}_2(\lambda_1, \lambda_2) = \rho_1^{[2]}(\lambda_1, \lambda_2) P_1^{[2]} + \rho_2^{[2]}(\lambda_1, \lambda_2) P_2^{[2]} + \rho_3^{[2]}(\lambda_1, \lambda_2) P_3^{[2]}, \quad (31)$$

where the operators $P_k^{[2]}$ are chosen as,

$$P_1^{[2]} = \begin{array}{c} \bullet \\ \curvearrowright \\ \bullet \end{array}, \quad P_2^{[2]} = \begin{array}{c} \bullet \\ \diagdown \diagup \\ \bullet \end{array}, \quad P_3^{[2]} = \begin{array}{c} \bullet \quad \bullet \\ \diagdown \diagup \\ \bullet \quad \bullet \end{array}, \quad (32)$$

and the functions $\rho_k^{[2]}(\lambda_1, \lambda_2)$ are to be determined. It is worth to note that we only need three linearly independent operators/states which can be seen as tensor anti-symmetric in the three connected indices (black dots) and symmetric in the other two. Alternatively, we can consider the operators $P_j^{[2]}$ as vector in $[\bar{3}]^{\otimes 4} \otimes [3]$, with the indices $i_1, i_2, i_3, r_1, s_1 = 1, 2, 3$ assigned to the dots, such that e.g. for $P_1^{[2]}$ we have

$$\left(P_1^{[2]}\right)_{i_1, i_2, i_3, r_1}^{s_1} := \epsilon_{i_1, i_2, i_3} \cdot \delta_{r_1}^{s_1} \equiv \begin{array}{c} i_1 \quad r_1 \\ \curvearrowright \quad | \\ i_2 \quad \rightarrow \quad | \\ \curvearrowright \quad | \\ i_3 \quad s_1 \end{array} . \quad (33)$$

Note that upper indices refer to states from $[3]$ and lower indices refer to states from $[\bar{3}]$. And furthermore, this object has the right transformation properties, namely invariance under $SU(3)$, because for arbitrary $g \in SU(3)$ we have $g^* \otimes g^* \otimes g^* \cdot \epsilon = \det(g^*)\epsilon = \epsilon$ and $g^* \otimes g \cdot \text{id} = \text{id}$. For convenience we have chosen to work with operators which resemble the usual identity, permutation and Temperley-Lieb defined before and that after partial anti-symmetrization reduce to the combination of identity, permutation and Temperley-Lieb. This way, the density operator (31) would nicely reduce to the usual density operator (27) as $D_2(\lambda_1, \lambda_2) = (2\rho_1^{[2]} + \rho_3^{[2]})I + (2\rho_2^{[2]} - \rho_3^{[2]})P_{12}$ thanks to the properties (17).

Using the above representation of the density operator (31), equation (24) implies the following set of functional equations

$$\begin{pmatrix} \rho_1^{[2]}(\lambda_1, \lambda_2) \\ \rho_2^{[2]}(\lambda_1, \lambda_2) \\ \rho_3^{[2]}(\lambda_1, \lambda_2) \end{pmatrix} = A^{[2]}(\lambda) \cdot \begin{pmatrix} \rho_1^{[2]}(\lambda_1 + 1, \lambda_2) \\ \rho_2^{[2]}(\lambda_1 + 1, \lambda_2) \\ \rho_3^{[2]}(\lambda_1 + 1, \lambda_2) \end{pmatrix}, \quad \lambda_1 = u_i, \quad (34)$$

where $\lambda = \lambda_1 - \lambda_2$ and the matrix $A^{[2]}(\lambda)$ is given by,

$$A^{[2]}(\lambda) = \begin{pmatrix} \frac{(-1+3\lambda+\lambda^2)}{\lambda(\lambda+3)} & \frac{(-2+2\lambda+\lambda^2)}{\lambda(\lambda+3)} & \frac{1}{\lambda+3} \\ \frac{3}{\lambda(\lambda+3)} & \frac{-(-3+\lambda+\lambda^2)}{\lambda(\lambda+3)} & \frac{\lambda}{\lambda+3} \\ 0 & \frac{-(-1+\lambda)}{\lambda} & 0 \end{pmatrix}.$$

These equations can be disentangled by the transformation matrix

$$\begin{pmatrix} 1 \\ \omega_{33}(\lambda_1, \lambda_2) \\ \omega_{\bar{3}3}(\lambda_1 - 1, \lambda_2) \end{pmatrix} = \begin{pmatrix} 18 & 6 & 6 \\ 6 & 18 & -6 \\ 6 & -6 & 18 \end{pmatrix} \cdot \begin{pmatrix} \rho_1^{[2]}(\lambda_1, \lambda_2) \\ \rho_2^{[2]}(\lambda_1, \lambda_2) \\ \rho_3^{[2]}(\lambda_1, \lambda_2) \end{pmatrix}, \quad (35)$$

which expresses the normalization condition and the partial antisymmetrization in the lower and upper two semi-infinite lines of the density operator represented in Figure 9. Here, the properties (19-20) were used.

In terms of the above functions, the functional equation becomes,

$$\omega_{33}(\lambda_1, \lambda_2) = \frac{(\lambda - 1)(\lambda + 1)}{\lambda(\lambda + 3)} \omega_{\bar{3}3}(\lambda_1, \lambda_2) + \frac{1}{\lambda}, \quad (36)$$

$$\begin{aligned} \omega_{\bar{3}3}(\lambda_1 - 1, \lambda_2) &= -\frac{(\lambda - 1)(\lambda + 3)}{\lambda(\lambda + 3)} \omega_{33}(\lambda_1 + 1, \lambda_2) - \frac{(\lambda - 1)(\lambda + 2)}{\lambda(\lambda + 3)} \omega_{\bar{3}3}(\lambda_1, \lambda_2) \\ &\quad + \frac{\lambda - 1}{\lambda}, \end{aligned} \quad (37)$$

for $\lambda_1 = u_i$ and arbitrary λ_2 .

5.1.1 Zero temperature solution

At zero temperature, the above functional equations hold for arbitrary λ_1 . This is because at zero temperature one has to take the Trotter limit ($N \rightarrow \infty$) and therefore the horizontal spectral parameters u_i can take an infinite number of continuous values.

Therefore, we solve Eq.(36) for $\omega_{\bar{3}3}(\lambda_1, \lambda_2)$ and insert this into Eq. (37), resulting in

$$\frac{\omega_{33}(\lambda_1 + 1, \lambda_2)}{\lambda(\lambda + 2)} + \frac{\omega_{33}(\lambda_1, \lambda_2)}{(\lambda - 1)(\lambda + 1)} + \frac{\omega_{33}(\lambda_1 - 1, \lambda_2)}{\lambda(\lambda - 2)} = \frac{\lambda^2 + 2}{(\lambda^2 - 4)(\lambda^2 - 1)}. \quad (38)$$

In addition, at zero temperature the bi-variate function $\omega_{33}(\lambda_1, \lambda_2)$ turns into a single-variable function $\omega_{33}(\lambda_1 - \lambda_2)$ depending only on the difference of the

arguments, which allows us to define

$$\sigma(\lambda) = \frac{\omega_{33}(\lambda)}{(\lambda-1)(\lambda+1)}. \quad (39)$$

Therefore, equation (38) can be written as

$$\sigma(\lambda+1) + \sigma(\lambda) + \sigma(\lambda-1) = \frac{\lambda^2 + 2}{(\lambda-2)(\lambda-1)(\lambda+1)(\lambda+2)}, \quad (40)$$

whose solution obtained via Fourier transform is given by,

$$\sigma(\lambda) = -\frac{d}{d\lambda} \log \left\{ \frac{\Gamma(1 + \frac{1}{3} + \frac{\lambda}{3})\Gamma(1 - \frac{\lambda}{3})}{\Gamma(1 + \frac{1}{3} - \frac{\lambda}{3})\Gamma(1 + \frac{\lambda}{3})} \right\} - \frac{1}{\lambda^2 - 1}. \quad (41)$$

Having this solution we obtain $\omega_{33}(\lambda_1, \lambda_2)$. Taking the homogeneous limit ($\lambda_k \rightarrow 0$), we obtain

$$\omega_{33}(0, 0) = -\sigma(0) = 1 - \frac{\pi}{3\sqrt{3}} - \log 3 \approx -0.70321207674618, \quad (42)$$

which is precisely the ground state energy, as expected [22, 23], which is a special correlation function. The α_{33} coefficient in the density operator (27) is obtained from (29) and (42) such that,

$$\alpha_{33}(0, 0) = \frac{1}{24} \left[2 - \frac{\pi}{\sqrt{3}} - 3 \log 3 \right] \approx -0.12956817625994. \quad (43)$$

5.1.2 Properties of the two-point function

Differently from $SU(2)$, in the higher-rank case of $SU(3)$ the function $\omega_{33}(\lambda)$ is a generating function of special combinations of modified ζ functions (Hurwitz' zeta function).

We define a function $G(\lambda)$ as follows

$$\begin{aligned} G(\lambda) &= \frac{\omega_{33}(\lambda) + 1}{\lambda^2 - 1} \\ &= \frac{1}{3} \left[\psi_0 \left(1 - \frac{\lambda}{3} \right) - \psi_0 \left(1 + \frac{1}{3} - \frac{\lambda}{3} \right) + \psi_0 \left(1 + \frac{\lambda}{3} \right) - \psi_0 \left(1 + \frac{1}{3} + \frac{\lambda}{3} \right) \right], \end{aligned} \quad (44)$$

where $\psi_0(z)$ is the digamma function $\psi_0(z) = \frac{d}{dz} \log \Gamma(z)$.

Expanding $G(\lambda)$ in a power series we obtain

$$3G(\lambda) = 2 \sum_{k=0}^{\infty} \frac{1}{2k!} \left[\psi_{2k}(1) - \psi_{2k}\left(1 + \frac{1}{3}\right) \right] \left(\frac{\lambda}{3}\right)^{2k}, \quad (45)$$

where now $\psi_m(\lambda)$ is the polygamma function.

We can use the fact that $\psi_m(z) = (-1)^{m+1}(m)!\zeta(m+1, z)$, where $\zeta(m, z)$ is the modified zeta function defined as

$$\zeta(m, a) = \sum_{k=0}^{\infty} \frac{1}{(k+a)^m}, \quad (46)$$

and re-write expression (45) as

$$3G(\lambda) = 2 \sum_{k=1}^{\infty} \left[\zeta(2k+1, 1) - \zeta\left(2k+1, 1 + \frac{1}{3}\right) \right] \left(\frac{\lambda}{3}\right)^{2k} + 2 \left[\psi_0(1) - \psi_0\left(1 + \frac{1}{3}\right) \right]. \quad (47)$$

Then we see that $G(\lambda)$ is a generating function of differences of the modified zeta function $\zeta(2k+1, 1) - \zeta(2k+1, 1 + \frac{1}{3})$, albeit not of the modified zeta function itself.

5.2 Computation of the three-sites density operator

In the three-sites case, the density operator can be written as a superposition of 11 linearly independent operators as follows,

$$\mathfrak{D}_3(\lambda_1, \lambda_2, \lambda_3) = \sum_{k=1}^{11} \rho_k^{[3]}(\lambda_1, \lambda_2, \lambda_3) P_k^{[3]} \quad (48)$$

where the operators $P_k^{[3]}$ are chosen as,

$$\begin{aligned} P_1^{[3]} &= \begin{array}{c} \bullet \quad \bullet \quad \bullet \\ \downarrow \quad \downarrow \quad \downarrow \\ \bullet \quad \bullet \quad \bullet \end{array}, & P_2^{[3]} &= \begin{array}{c} \bullet \quad \bullet \quad \bullet \\ \downarrow \quad \downarrow \quad \downarrow \\ \bullet \quad \bullet \quad \bullet \end{array}, & P_3^{[3]} &= \begin{array}{c} \bullet \quad \bullet \quad \bullet \\ \downarrow \quad \downarrow \quad \downarrow \\ \bullet \quad \bullet \quad \bullet \end{array}, & P_4^{[3]} &= \begin{array}{c} \bullet \quad \bullet \quad \bullet \\ \downarrow \quad \downarrow \quad \downarrow \\ \bullet \quad \bullet \quad \bullet \end{array}, \\ P_5^{[3]} &= \begin{array}{c} \bullet \quad \bullet \quad \bullet \\ \downarrow \quad \downarrow \quad \downarrow \\ \bullet \quad \bullet \quad \bullet \end{array}, & P_6^{[3]} &= \begin{array}{c} \bullet \quad \bullet \quad \bullet \\ \downarrow \quad \downarrow \quad \downarrow \\ \bullet \quad \bullet \quad \bullet \end{array}, & P_7^{[3]} &= \begin{array}{c} \bullet \quad \bullet \quad \bullet \\ \downarrow \quad \downarrow \quad \downarrow \\ \bullet \quad \bullet \quad \bullet \end{array}, & P_8^{[3]} &= \begin{array}{c} \bullet \quad \bullet \quad \bullet \\ \downarrow \quad \downarrow \quad \downarrow \\ \bullet \quad \bullet \quad \bullet \end{array}, \end{aligned}$$

$$P_9^{[3]} = \begin{array}{c} \bullet \quad \bullet \quad \bullet \\ \diagdown \quad \diagup \quad \diagdown \\ \bullet \quad \bullet \quad \bullet \\ \diagup \quad \diagdown \quad \diagup \\ \bullet \quad \bullet \quad \bullet \end{array}, \quad P_{10}^{[3]} = \begin{array}{c} \bullet \quad \bullet \quad \bullet \\ \diagdown \quad \diagup \quad \diagdown \\ \bullet \quad \bullet \quad \bullet \\ \diagup \quad \diagdown \quad \diagup \\ \bullet \quad \bullet \quad \bullet \end{array}, \quad P_{11}^{[3]} = \begin{array}{c} \bullet \quad \bullet \quad \bullet \\ \diagdown \quad \diagup \quad \diagdown \\ \bullet \quad \bullet \quad \bullet \\ \diagup \quad \diagdown \quad \diagup \\ \bullet \quad \bullet \quad \bullet \end{array},$$

and the functions $\rho_k^{[3]}(\lambda_1, \lambda_2)$ are to be determined. Like in the two-point case, we have conveniently chosen the operators as tensor products of the totally anti-symmetric tensor and the identity/Kronecker symbol to resemble identity, permutation and Temperley-Lieb acting in different spaces as $I, P_{12}, P_{23}, P_{13}, P_{12}P_{23}, P_{23}P_{12}, E_{12}, E_{13}, E_{12}P_{23}, P_{23}E_{12}$ plus one operator which due to symmetry must allow for a symmetric combination of the indices in the first column of dots/indices as given in $P_8^{[3]}$. We have checked that the above chosen operators are indeed linearly independent. Again, after partial anti-symmetrization, the density operator (48) can be reduced to the usual density operator for three-sites $D_3(\lambda_1, \lambda_2, \lambda_3) = (2\rho_1^{[3]} - \rho_7^{[3]} - \rho_9^{[3]})I + (2\rho_2^{[3]} + \rho_7^{[3]})P_{12} + (2\rho_3^{[3]} - \rho_{10}^{[3]} - \rho_{11}^{[3]})P_{23} + (2\rho_4^{[3]} - \rho_8^{[3]} + \rho_9^{[3]})P_{13} + (2\rho_5^{[3]} + \rho_8^{[3]} + \rho_{10}^{[3]})P_{12}P_{23} + (2\rho_6^{[3]} + \rho_{11}^{[3]})P_{23}P_{12}$ by means of the use of the properties (17).

Analogously to the two-sites case, the operator $P_j^{[3]}$ can be seen as vector with the indices $i_1, i_2, i_3, r_1, r_2, s_1, s_2 = 1, 2, 3$ assigned to the dots, such that e.g. for $P_1^{[3]}$ we have

$$\left(P_1^{[3]}\right)_{i_1, i_2, i_3, r_1, r_2}^{s_1, s_2} := \epsilon_{i_1, i_2, i_3} \delta_{r_1}^{s_1} \delta_{r_2}^{s_2} \equiv \begin{array}{c} i_1 \quad r_1 \quad r_2 \\ \bullet \quad \bullet \quad \bullet \\ \diagdown \quad \diagup \quad \diagdown \\ i_2 \quad \bullet \quad \bullet \\ \bullet \quad \bullet \quad \bullet \\ \diagup \quad \diagdown \quad \diagup \\ i_3 \quad s_1 \quad s_2 \end{array}, \quad (49)$$

which shows that the computation for three-sites goes along the same lines as in the two-sites case, we just have to deal with a large number of extended operators $P_j^{[3]}$.

Inserting the above expansion of the density operator (48) into equation (24) yields the set of functional equations

$$\vec{\rho}(\lambda_1, \lambda_2, \lambda_3) = A^{[3]}(\lambda_1, \lambda_2) \cdot \vec{\rho}(\lambda_1 + 1, \lambda_2, \lambda_3), \quad (50)$$

where $\vec{\rho}(\lambda_1, \lambda_2, \lambda_3)$ is a 11 dimensional vector whose entries are the expansion coefficients $\rho_k^{[3]}(\lambda_1, \lambda_2, \lambda_3)$ for $k = 1, \dots, 11$ and the matrix $A^{[3]}(\lambda_1, \lambda_2, \lambda_3)$, which is obtained from the action of the linear operator $\mathfrak{A}_3(\lambda_1, \lambda_2, \lambda_3)$ (25) on the mixed density operator (48), is given in appendix B.

For convenience of the presentation of the results, we define the intermediate auxiliary functions $f_k(\lambda_1, \lambda_2, \lambda_3) = (P_k^{[3]})^t \cdot \mathfrak{D}_3(\lambda_1, \lambda_2, \lambda_3)$ by

$$\vec{f}(\lambda_1, \lambda_2, \lambda_3) = M \cdot \vec{\rho}(\lambda_1, \lambda_2, \lambda_3), \quad (51)$$

where the matrix M is given by

$$M = \begin{pmatrix} 54 & 18 & 18 & 18 & 6 & 6 & 18 & 6 & 18 & 6 & 6 \\ 18 & 54 & 6 & 6 & 18 & 18 & -18 & -6 & 6 & -6 & -6 \\ 18 & 6 & 54 & 6 & 18 & 18 & 6 & -6 & 6 & 18 & 18 \\ 18 & 6 & 6 & 54 & 18 & 18 & 6 & 18 & -18 & -6 & -6 \\ 6 & 18 & 18 & 18 & 54 & 6 & -6 & -18 & -6 & -18 & 6 \\ 6 & 18 & 18 & 18 & 6 & 54 & -6 & 6 & -6 & 6 & -18 \\ 18 & -18 & 6 & 6 & -6 & -6 & 54 & -6 & 6 & 18 & 18 \\ 6 & -6 & -6 & 18 & -18 & 6 & -6 & 54 & -6 & 6 & 6 \\ 18 & 6 & 6 & -18 & -6 & -6 & 6 & -6 & 54 & 18 & 18 \\ 6 & -6 & 18 & -6 & -18 & 6 & 18 & 6 & 18 & 54 & 6 \\ 6 & -6 & 18 & -6 & 6 & -18 & 18 & 6 & 18 & 6 & 54 \end{pmatrix}. \quad (52)$$

The equations (50) can be disentangled by making a suitable transformation. This can be done by using the reduction properties like the intertwining symmetry, the partial trace and so on in order to identify 8 linearly independent combinations of the functions $f_k(\lambda_1, \lambda_2, \lambda_3)$ as two-site functions (or simpler) and 3 remaining combinations as true three-site functions. Therefore, the suitable functions can be

written in terms of the auxiliary functions as follows,

$$\begin{aligned}
1 &= f_1, \\
\omega_{33}(\lambda_1, \lambda_2) &= f_2, \\
\omega_{\bar{3}3}(\lambda_1 - 1, \lambda_2) &= f_7, \\
\omega_{33}(\lambda_1, \lambda_3)(1 - y^2) &= f_3 + yf_6 - yf_5 - y^2f_4, \\
\omega_{\bar{3}3}(\lambda_1 - 1, \lambda_3)(1 - y)(2 + y) &= f_7 - (y + 2)f_{10} + (y - 1)f_{11} - (y - 1)(y + 2)f_9, \\
\omega_{33}(\lambda_1, \lambda_2)(1 - x^2)(1 - (x - y)^2) &= (1 - (x - y)^2)f_3 + x(x - 2y)f_4 \\
&+ x(-1 + xy - y^2)f_5 + x(1 - xy + y^2)f_6 + x(x - y)(-2 + x^2 - xy)f_2, \\
\omega_{\bar{3}3}(\lambda_1 - 1, \lambda_2)(1 - x)(2 + x)(1 - (x - y)^2) &= \\
(1 - (-1 + x)(x - y) - (2 + x)(x - y) + (-1 + x)(2 + x)(x - y)^2)f_7 \\
&+ (2 - y - y^2)f_9 + (2 + y)(-1 + x^2 + y - x(1 + y))f_{10} \\
&+ (-1 + y)(1 - x^2 + x(-2 + y) + 2y)f_{11}, \\
\omega_{33}(\lambda_2, \lambda_3) &= f_3, \\
F_1(\lambda_1, \lambda_2, \lambda_3) &= 2x(2 + x)y(2 + y)f_1 + 2x(2 + x)(2 + y)f_2 \\
&+ 2(2 + x)y(2 + y)f_4 + 2(2 + x)(2 + y)f_5, \\
F_2(\lambda_1, \lambda_2, \lambda_3) &= 2(-2 - y - x(2 + y) + x(2 + x)y(2 + y))f_1 \\
&- 2(-1 + x + x^2)(2 + y)f_2 + 2(1 + x)(2 + y)f_3 \\
&+ 2(1 + x + (2 + x)y - (2 + x)y(2 + y))f_4 - 2(1 + x + 2y + xy)f_5 \\
&+ 2(2 + y)f_6 - 2(-2 - y + xy + x^2(1 + y))f_7 + 2(1 + x - y)f_8 \\
&- 2(1 + x)(-2 + y + y^2)f_9 - 2(1 + x)(2 + y)f_{10} - 2xf_{11}, \\
F_3(\lambda_1, \lambda_2, \lambda_3) &= 2(x^2 - 1)(y^2 - 1)f_1 + 2(x^2 - 1)(1 + y)f_7 \\
&+ 2(1 + x)(y^2 - 1)f_9 + 2(1 + x)(1 + y)f_{10},
\end{aligned} \tag{53}$$

where $x = \lambda_1 - \lambda_3$ and $y = \lambda_1 - \lambda_2$ and the combination $f_1(\lambda_1, \lambda_2, \lambda_3)$ is the normalization condition (analogue of the total trace).

Substituting Eq. (51) in Eqs. (53) and solving the 11 linear equations for $\rho_1^{[3]}, \dots, \rho_{11}^{[3]}$ in terms of the known two-site functions and the yet unknown three-site functions F_1, F_2, F_3 , inserting these expressions into the functional equations (50) and using those for the two-point functions, reduces these to just three equations for the unknown functions. So the only remaining unknown functions are F_1, F_2, F_3 and satisfy a set of linear functional equations. By a suitable rescaling the coefficients of the occurring matrix take a very simple form

$$\begin{pmatrix} G_1(\lambda_1, \lambda_2, \lambda_3) \\ G_2(\lambda_1, \lambda_2, \lambda_3) \\ G_3(\lambda_1, \lambda_2, \lambda_3) \end{pmatrix} = \begin{pmatrix} 0 & 0 & 1 \\ 1 & 0 & 0 \\ 0 & 1 & 0 \end{pmatrix} \cdot \begin{pmatrix} G_1(\lambda_1 + 1, \lambda_2, \lambda_3) \\ G_2(\lambda_1 + 1, \lambda_2, \lambda_3) \\ G_3(\lambda_1 + 1, \lambda_2, \lambda_3) \end{pmatrix} + \begin{pmatrix} r(\lambda_1, \lambda_2, \lambda_3) \\ 0 \\ 0 \end{pmatrix}, \quad (54)$$

where $\lambda_1 = u_i$, and we have introduced for convenience the G_k -functions as,

$$\begin{aligned} G_1(\lambda_1, \lambda_2, \lambda_3) &= \frac{xy}{(x^2 - 1)(y^2 - 1)(x + 2)(y + 2)} F_1(\lambda_1, \lambda_2, \lambda_3), \\ G_2(\lambda_1, \lambda_2, \lambda_3) &= \frac{(x + 1)(y + 1)}{(x^2 - 1)(y^2 - 1)(x + 2)(y + 2)} F_2(\lambda_1, \lambda_2, \lambda_3), \\ G_3(\lambda_1, \lambda_2, \lambda_3) &= \frac{1}{(x^2 - 1)(y^2 - 1)} F_3(\lambda_1, \lambda_2, \lambda_3), \end{aligned} \quad (55)$$

and

$$\begin{aligned} r(\lambda_1, \lambda_2, \lambda_3) &= \frac{2(-1 + 2x^2 + 2y^2)}{(x^2 - 1)(y^2 - 1)} + \frac{2(x + y)}{(x^2 - 1)(y^2 - 1)} \omega_{33}(\lambda_2, \lambda_3) \\ &+ \frac{2(-1 + 3x + x^2 - 3y - 2xy + y^2 - 3xy^2 + 3y^3)}{x(x + 3)(x - y)(y^2 - 1)} \omega_{33}(\lambda_1, \lambda_3) \\ &- \frac{2(-1 - 3x + x^2 + 3x^3 + 3y - 2xy - 3x^2y + y^2)}{(x^2 - 1)(x - y)y(y + 3)} \omega_{33}(\lambda_1, \lambda_2). \end{aligned} \quad (56)$$

5.2.1 Zero temperature solution

At zero temperature, again, the above functional equations hold for arbitrary λ_1 . Since we have already obtained the solution for the two-site functions from Eq. (36-37), it only remains to solve equation (54).

However, equations (54) are more complicated to deal with, since one of the equations contains the inhomogeneity $r(\lambda_1, \lambda_2, \lambda_3)$ with a more complicated pole structure than in the two-site case. The inhomogeneity can be written in terms of digamma functions. This increases the complexity to obtain a closed solution for (54).

In order to avoid carrying out, for the time being, the Fourier transform of rational functions times digamma functions, we have chosen to write the solution in terms of convolutions. Eventually, the convolution integrals can be evaluated numerically as we will describe in what follows.

The problem can be significantly simplified by partially taking the homogeneous limit $\lambda_2 = \lambda_3 = 0$ and decoupling the equations (54) by the following transformation

$$\begin{aligned} g_0(\lambda_1) &= G_1(\lambda_1, 0, 0) + G_2(\lambda_1, 0, 0) + G_3(\lambda_1, 0, 0), \\ g_1(\lambda_1) &= G_1(\lambda_1, 0, 0) + wG_2(\lambda_1, 0, 0) + w^2G_3(\lambda_1, 0, 0), \\ g_{-1}(\lambda_1) &= G_1(\lambda_1, 0, 0) + w^{-1}G_2(\lambda_1, 0, 0) + w^{-2}G_3(\lambda_1, 0, 0), \end{aligned} \quad (57)$$

where $w = e^{\frac{2\pi i}{3}}$.

Therefore, the resulting equations become (we now set $\lambda_1 = \lambda$)

$$g_l(\lambda) = w^l g_l(\lambda + 1) + \varphi(\lambda), \quad (58)$$

where $l = 0, 1, -1$ and $\varphi(\lambda) = \lim_{\lambda_2, \lambda_3 \rightarrow 0} r(\lambda, \lambda_2, \lambda_3)$,

$$\begin{aligned} \varphi(\lambda) &= -\frac{12}{(\lambda^2 - 1)}\omega_{33}(\lambda, 0) - \frac{2}{(\lambda^2 - 1)^2}\omega'_{33}(\lambda, 0) + \frac{4\lambda}{(\lambda^2 - 1)^2}\omega_{33}(0, 0) \\ &\quad + \frac{2(4\lambda^4 + 6\lambda^3 - \lambda^2 - 6\lambda - 1)}{\lambda^2(\lambda^2 - 1)^2}, \end{aligned} \quad (59)$$

and the prime denotes the derivative with respect to the argument λ . Naturally the zero temperature solution for three-sites correlation must depend on the two-sites function $\omega_{33}(\lambda, 0)$ and its derivative $\omega'_{33}(\lambda, 0)$ via the $\varphi(\lambda)$, therefore the modified

zeta function would also appear explicitly in case of an analytic solution for the three-site correlation.

We use analyticity in the variable λ and Fourier transform the above equations. The resulting equations are algebraically solved for the Fourier coefficients and yield product expressions. Then, we Fourier transform back and find integrals of convolution type

$$g_l(\lambda) = \int_{-\infty}^{\infty} h_l(\lambda - \mu) \varphi(\mu) \frac{d\mu}{2\pi}, \quad (60)$$

where

$$h_l(z) = \int_{\mathbb{R}+i0} \frac{e^{ikz}}{1 - w^l e^k} dk. \quad (61)$$

The integral expression can be evaluated numerically at the homogeneous point $\lambda = 0$. This allows us to obtain the functions $G_i(0, 0, 0)$ (and derivatives of G_i at $(0, 0, 0)$) from which we compute $F_i(0, 0, 0)$ directly in the homogeneous limit. The function $F_1(0, 0, 0)$ is related to a simple three point correlation function $F_1(0, 0, 0) = 8\langle P_{12}P_{23} \rangle$. Using the result of the numerical evaluation of the integral equation (60), we obtain

$$\langle P_{12}P_{23} \rangle = 0.191368820116674 \quad (62)$$

The numerical data for finite lattices indicates an agreement with the infinite lattice result obtained from the solution of the functional equations, see Table 1. Although the numerical evaluation of the integral equations (60) is not computationally demanding, it would be desirable to have an exact analytical expression. As indicated above, the analytical calculation of the convolution integral requires the computation of the Fourier transform of a product of a rational function with a digamma functions which for the moment we leave as an exercise.

Length	$\omega_{33}(0, 0)$	$\langle P_{12}P_{23} \rangle$
$L = 3$	-1.0000000000000000	1.0000000000000000
$L = 6$	-0.767591879243998	0.309579305659537
$L = 9$	-0.731082881703061	0.239661721591669
$L \rightarrow \infty$	-0.703212076746182	0.191368820116674

Table 1: Comparison of numerical results from exact diagonalization for $L = 3, 6$ and Lanczos calculations for $L = 9$ sites with the analytical result in the thermodynamic limit.

6 Lack of factorization of the correlation functions

In the case of $SU(2)$ spin chains, it is well known that the correlation functions factorize in terms of two-site correlations [8, 26]. This property was useful in obtaining the correlation functions for the spin-1/2 system and also for higher-spin cases [20, 21].

Unfortunately, in the case of $SU(3)$ our attempts of solving Eq. (54) in terms of some naive factorized ansatz failed.

Besides, we have also investigated the factorization for finite Trotter number and (at first sight) surprisingly we realized that the three-point correlation functions are expressed in terms of the two-sites ($m = 2$) and also a three-sites ($m = 3$) emptiness formation probability (EFP). For instance, the following correlation function is given by

$$\begin{aligned}
\text{Tr} [P_{\text{singlet}} D_3(\lambda_1, \lambda_2, \lambda_3)] &= \frac{Q_3^{(s)}(\lambda_1, \lambda_2, \lambda_3)}{\Lambda_0^{(n)}(\lambda_1) \Lambda_0^{(n)}(\lambda_2) \Lambda_0^{(n)}(\lambda_3)} \\
&= 6 - 24 \left[\left(1 + \frac{1}{\lambda_{13}\lambda_{23}}\right) P_2(\lambda_1, \lambda_2) + \left(1 + \frac{1}{\lambda_{12}\lambda_{32}}\right) P_2(\lambda_1, \lambda_3) \right. \\
&\quad \left. + \left(1 + \frac{1}{\lambda_{21}\lambda_{31}}\right) P_2(\lambda_2, \lambda_3) \right] + 60 P_3(\lambda_1, \lambda_2, \lambda_3), \quad (63)
\end{aligned}$$

where $P_{singlet}$ is the $SU(3)$ singlet projector and

$$P_2(\lambda_1, \lambda_2) = \left[D_2^{(3,3)}(\lambda_1, \lambda_2) \right]_{11}^{11} = \frac{Q_2(\lambda_1, \lambda_2)}{\Lambda_0^{(n)}(\lambda_1) \Lambda_0^{(n)}(\lambda_2)}, \quad (64)$$

$$P_3(\lambda_1, \lambda_2, \lambda_3) = \left[D_3^{(3,3)}(\lambda_1, \lambda_2, \lambda_3) \right]_{111}^{111} = \frac{Q_3(\lambda_1, \lambda_2, \lambda_3)}{\Lambda_0^{(n)}(\lambda_1) \Lambda_0^{(n)}(\lambda_2) \Lambda_0^{(n)}(\lambda_3)}, \quad (65)$$

and $Q_m(\lambda_1, \dots, \lambda_m)$ are polynomials of known degree in each variable and $\Lambda_0^{(n)}(\lambda)$ is again the leading eigenvalue of the quantum transfer matrix but with finite Trotter number N . It is worth to emphasize that $P_3(\lambda_1, \lambda_2, \lambda_3)$ cannot be written only in terms of the $P_2(\lambda_i, \lambda_j)$, so it does not factorize in terms of the two-point emptiness formation probability. The correlations for the case $m = 4$ also do not factorize only in terms of $m = 2, 3$ correlators, but require one four-point function, e.g. the emptiness formation probability of four-sites $P_4(\lambda_1, \lambda_2, \lambda_3, \lambda_4)$.

Therefore, this might indicate that the correlations of high rank spin chains cannot be factorized only in terms of two-point functions, which brings an additional degree of difficulty in order to push the calculation to correlations at longer distances.

7 Conclusions

We have formulated a consistent approach to deal with short-distance correlation functions of the $SU(n)$ spin chains for $n > 2$ at zero and finite-temperature. The fact that the model does not have crossing symmetry turned the derivation of functional equations for the correlation functions much more challenging than in the $SU(2)$ case. The difficulties which arise were circumvented by working with generalized density operators of two types. These operators not only contain the physically interesting correlation functions, but many other correlations with mixed representations. In this sense, this approach exploits the full $SU(n)$ structure.

We considered in detail the special case of $SU(3)$ for two- and three-site correlations ($m = 2, 3$). We used the discrete functional equations to obtain the equations which fix the two-point correlation functions. Besides, we have solved the equations via Fourier transform at zero temperature and its solutions are explicitly given in terms of digamma functions. The correlation function for the local Hamiltonian gives the ground state energy as expected.

In addition, we considered the case of three-point correlations. The computation is much more involved in this case, since the dimension of the singlet space of the generalized mixed density operator is 11. Therefore, we had to obtain this large number of equations and by appropriate identification of two and three-site functions, we reduced these 11 equations to just 3 decoupled functional equations. We derived an integral expression of convolution type for the remaining three-point functions. The integrals were evaluated numerically giving the result for three-point correlation functions in the thermodynamical limit. We compared the infinite system size result with the result obtained for very finite lattices $L = 3, 6$ and 9 , which shows the correct trend.

Moreover, we have also investigated the possibility of the three-point function to be factorized in terms of two-point correlations. Our attempts were based on the proposition of an ansatz for the solution of the functional equations for the three-point functions (54), which always led us to contradictions of the proposed ansatz, indicating that the factorized ansatz does not apply to the model. Additionally, we investigated the possibility of factorization at finite Trotter number. At finite Trotter number the correlators are rational functions, which allowed us to realize that three-point correlations can be decomposed in terms of two-point function and an additional three-point function. Therefore, this is also another indication of lack of factorization.

In this work, we have obtained the first results about the correlation functions

of Yang-Baxter integrable $SU(n)$ quantum spin chains. We obtained analytical and numerical results for nearest ($m = 2$) and next-nearest ($m = 3$) correlators. We would still like to obtain an analytical evaluation of the convolution integrals for the $m = 3$ case. It is completely open, how to solve the functional equation for the cases of $m \geq 4$. In the general case of $SU(n)$ ($n > 3$), we have only the solution for $m = 2$. Of course, here it would also be desirable to obtain the explicit functional equations for $m = 3$ and its solution, at least for $SU(4)$. Another interesting goal is the explicit evaluation of the correlations at finite temperature. In order to do that, we have to derive the non-linear integral equation for the generalized quantum transfer matrix and more challenging we have to devise a way to evaluate the three-point functions at finite temperature. The standard trick for the evaluation of the two-point function at finite temperature comprises the derivative of the leading eigenvalue with respect to some inhomogeneity parameter [14], however this trick cannot be applied to three-point correlations. The above mentioned issues are currently under investigation.

Acknowledgments

G.A.P. Ribeiro thanks the São Paulo Research Foundation (FAPESP) for financial support through the grants 2017/16535-1 and 2015/01643-8. He also acknowledges the hospitality of Bergische Universität Wuppertal. This work has been carried out within the DFG research unit Correlations in Integrable Quantum Many-Body Systems (FOR2316).

Note added: After our paper appeared on the arXiv, we became aware of the related preprint [27].

Appendix A: Reduction of \mathbb{D}_m to \mathbb{D}_{m-1}

We may apply the completely anti-symmetric tensor ϵ to any of the bunches of n semi-infinite lines of \mathbb{D}_m . Then by use of the properties (13) the anti-symmetrizer can be moved towards the far left resulting in \mathbb{D}_{m-1} times some proportionality factor. This is illustrated in Figure A.1 for the case $m = 2$ and $SU(3)$.

We like to point out that repeated applications of anti-symmetrizers to \mathbb{D}_m yield $\mathbb{D}_{\tilde{m}}$ with arbitrary $\tilde{m} (\leq m)$. Note, the application of m times the anti-symmetric tensor ϵ removes all degrees of freedom and serves as the normalization of \mathbb{D}_m .

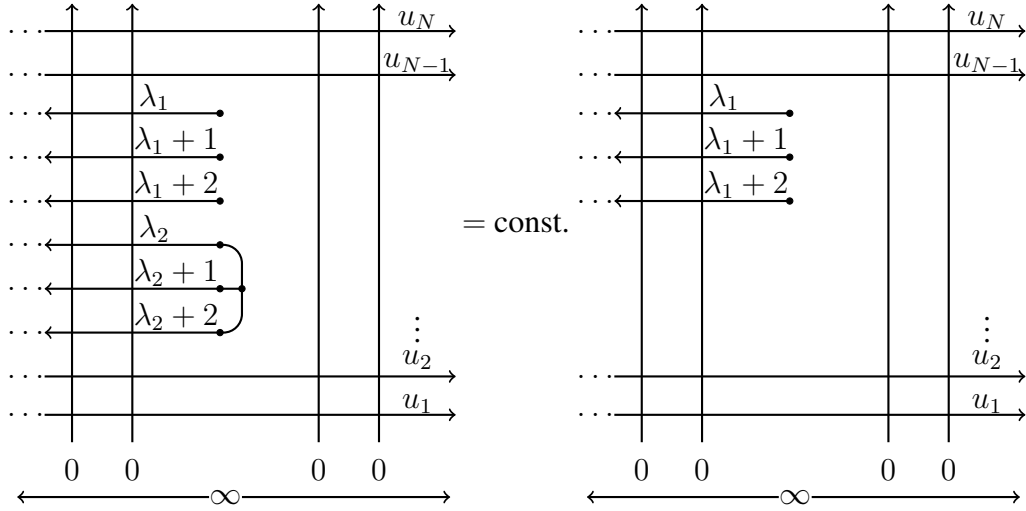


Figure A.1: Graphical illustration of the reduction property of two-sites to one site correlation. This property can be iterated until we reach the normalization condition of the generalized density operator $\mathbb{D}_2(\lambda_1, \lambda_2)$.

Appendix B: The matrix $A^{[3]}$ for the three point case.

Here we give the 11×11 matrix $A^{[3]}$ which defines the system of functional equations for the functions $\rho_k^{[3]}(\lambda_1, \lambda_2, \lambda_3)$. This was obtained by replacing (48) into equation (24), along the same lines as in the two-sites case.

$$A^{[3]} = \begin{pmatrix} a_{1,1} & a_{1,2} & a_{1,3} & a_{1,4} & a_{1,5} & a_{1,6} & a_{1,7} & a_{1,8} & a_{1,9} & a_{1,10} & a_{1,11} \\ a_{2,1} & a_{2,2} & a_{2,3} & a_{2,4} & a_{2,5} & a_{2,6} & a_{2,7} & a_{2,8} & a_{2,9} & a_{2,10} & a_{2,11} \\ a_{3,1} & a_{3,2} & a_{3,3} & a_{3,4} & a_{3,5} & a_{3,6} & a_{3,7} & a_{3,8} & a_{3,9} & a_{3,10} & a_{3,11} \\ a_{4,1} & 0 & a_{4,3} & a_{4,4} & a_{4,5} & a_{4,6} & 0 & a_{4,8} & a_{4,9} & 0 & a_{4,11} \\ a_{5,1} & a_{5,2} & a_{5,3} & a_{5,4} & a_{5,5} & a_{5,6} & a_{5,7} & a_{5,8} & a_{5,9} & a_{5,10} & a_{5,11} \\ a_{6,1} & a_{6,2} & a_{6,3} & a_{6,4} & a_{6,5} & a_{6,6} & 0 & a_{6,8} & a_{6,9} & 0 & a_{6,11} \\ 0 & a_{7,2} & 0 & a_{7,4} & a_{7,5} & a_{7,6} & 0 & a_{7,8} & 0 & 0 & 0 \\ 0 & a_{8,2} & 0 & a_{8,4} & a_{8,5} & a_{8,6} & 0 & a_{8,8} & 0 & 0 & 0 \\ 0 & 0 & 0 & a_{9,4} & a_{9,5} & 0 & 0 & a_{9,8} & 0 & 0 & 0 \\ 0 & 0 & 0 & a_{10,4} & a_{10,5} & 0 & 0 & a_{10,8} & 0 & 0 & 0 \\ 0 & a_{11,2} & 0 & a_{11,4} & a_{11,5} & a_{11,6} & 0 & a_{11,8} & 0 & 0 & 0 \end{pmatrix} \quad (\text{B.1})$$

where the non-trivial matrix elements are written as follows,

$$\begin{aligned} a_{1,1} &= \frac{(-1 + 3x + x^2)(-1 + 3y + y^2)}{x(3+x)y(3+y)}, a_{1,2} = \frac{(-1 + 3x + x^2)(-2 + 2y + y^2)}{x(3+x)y(3+y)}, \\ a_{1,3} &= -\frac{3}{x(3+x)y(3+y)}, a_{1,4} = \frac{(1+y)(-8 + 3x + 2x^2 - 2y + 2xy + x^2y)}{x(3+x)y(3+y)}, \\ a_{1,5} &= \frac{(1+y)(-7 + x^2 - 3y - xy)}{x(3+x)y(3+y)}, a_{1,6} = \frac{-3 + y + y^2}{x(3+x)y(3+y)}, \\ a_{1,7} &= \frac{-1 + 3x + x^2}{x(3+x)(3+y)}, a_{1,8} = \frac{-1 + 3x + x^2 + y + 3xy + x^2y}{x(3+x)y(3+y)}, \end{aligned} \quad (\text{B.2})$$

$$\begin{aligned}
a_{1,9} &= \frac{1+3x+xy}{x(3+x)(3+y)}, a_{1,10} = -\frac{-1+x^2-xy}{x(3+x)y(3+y)}, a_{1,11} = -\frac{y}{x(3+x)(3+y)}, \\
a_{2,1} &= \frac{3(-1+3x+x^2)}{x(3+x)y(3+y)}, a_{2,2} = -\frac{(-1+3x+x^2)(-3+y+y^2)}{x(3+x)y(3+y)}, \\
a_{2,3} &= -\frac{-1+3y+y^2}{x(3+x)y(3+y)}, a_{2,4} = \frac{2(1+y)}{x(3+x)y(3+y)}, a_{2,5} = \frac{(1+y)^2}{x(3+x)y(3+y)}, \\
a_{2,6} &= -\frac{-2+2y+y^2}{x(3+x)y(3+y)}, a_{2,7} = \frac{(-1+3x+x^2)y}{x(3+x)(3+y)}, a_{2,8} = -\frac{-1+y}{x(3+x)y(3+y)}, \\
a_{2,9} &= \frac{1+3x+xy}{x(3+x)y(3+y)}, a_{2,10} = -\frac{-1+x^2-xy}{x(3+x)(3+y)}, a_{2,11} = -\frac{1}{x(3+x)(3+y)}, \\
a_{3,1} &= -\frac{3}{x(3+x)y(3+y)}, a_{3,2} = -\frac{3(2+y)}{x(3+x)y(3+y)}, \\
a_{3,3} &= \frac{-3x-3y+7xy+3x^2y+3xy^2+x^2y^2}{x(3+x)y(3+y)}, a_{3,4} = -\frac{-6+6x+3x^2-6y-2xy}{x(3+x)y(3+y)}, \\
a_{3,5} &= \frac{3-6x-3x^2+6y+6xy+x^2y+3y^2+4xy^2+x^2y^2}{x(3+x)y(3+y)}, \\
a_{3,6} &= \frac{-3x-6y+6xy+3x^2y-3y^2+2xy^2+x^2y^2}{x(3+x)y(3+y)}, \\
a_{3,7} &= \frac{3}{x(3+x)(3+y)}, a_{3,8} = -\frac{-3+3y+4xy+x^2y}{x(3+x)y(3+y)}, a_{3,9} = -\frac{1}{x(3+y)}, \\
a_{3,10} &= \frac{-3+3x^2+x^2y}{x(3+x)y(3+y)}, a_{3,11} = \frac{y}{x(3+y)}, \\
a_{4,1} &= \frac{3}{x(3+x)}, a_{4,3} = -\frac{-9+x^2-3y-2xy}{x(3+x)y(3+y)}, \\
a_{4,4} &= -\frac{-3x-x^2-9y+3xy+3x^2y-3y^2+xy^2+x^2y^2}{x(3+x)y(3+y)}, \\
a_{4,5} &= -\frac{-3+x-y}{xy(3+y)}, a_{4,6} = \frac{3+x-y}{(3+x)y(3+y)}, \\
a_{4,8} &= -\frac{9-3x-2x^2-6y+xy+2x^2y-3y^2+xy^2+x^2y^2}{x(3+x)y(3+y)}, \\
a_{4,9} &= \frac{-3-x+y+3xy+xy^2}{(3+x)y(3+y)}, a_{4,11} = \frac{3+x-y}{(3+x)(3+y)}, \\
a_{5,1} &= -\frac{3}{x(3+x)(3+y)}, a_{5,2} = \frac{3}{x(3+x)(3+y)}, \\
a_{5,3} &= \frac{-3+8x+3x^2+x^2y-xy^2}{x(3+x)y(3+y)}, a_{5,4} = -\frac{-1+y}{xy(3+y)},
\end{aligned}$$

(B.3)

$$\begin{aligned}
a_{5,5} &= -\frac{3 - 8x - 3x^2 - 3y + 2xy + 2x^2y + 2xy^2 + x^2y^2}{x(3+x)y(3+y)}, \\
a_{5,6} &= \frac{1}{xy(3+y)}, a_{5,7} = \frac{3y}{x(3+x)(3+y)}, \\
a_{5,8} &= \frac{6 - 7x - 3x^2 - 3y + 2xy + 2x^2y - 3y^2 + xy^2 + x^2y^2}{x(3+x)y(3+y)}, \\
a_{5,9} &= -\frac{1}{xy(3+y)}, a_{5,10} = \frac{-3 + 3x^2 + x^2y}{x(3+x)(3+y)}, a_{5,11} = \frac{1}{x(3+y)}, \\
a_{6,1} &= \frac{3}{x(3+x)y}, a_{6,2} = \frac{3}{x(3+x)y}, a_{6,3} = -\frac{-x - 9y + x^2y - 3y^2 - xy^2}{x(3+x)y(3+y)}, \\
a_{6,4} &= \frac{2+y}{(3+x)y(3+y)}, a_{6,5} = \frac{1}{(3+x)y(3+y)}, \\
a_{6,6} &= -\frac{-2x - 9y + 2xy + 2x^2y - 3y^2 + 2xy^2 + x^2y^2}{x(3+x)y(3+y)}, \\
a_{6,8} &= \frac{1}{(3+x)y(3+y)}, a_{6,9} = \frac{1+3x-3y}{(3+x)y(3+y)}, a_{6,11} = \frac{-1+3y+xy}{(3+x)(3+y)}, \\
a_{7,2} &= -\frac{(-1+3x+x^2)(-1+y)}{x(3+x)y}, a_{7,4} = -\frac{-8+6x+3x^2-4y-xy}{x(3+x)y(3+y)}, \\
a_{7,5} &= -\frac{-1-8y+x^2y-3y^2-xy^2}{x(3+x)y(3+y)}, a_{7,6} = -\frac{-1+y}{x(3+x)y}, \\
a_{7,8} &= \frac{7-6x-3x^2-5y+xy+x^2y-2y^2+2xy^2+x^2y^2}{x(3+x)y(3+y)}, \\
a_{8,2} &= \frac{3}{x(3+x)}, a_{8,4} = -\frac{3(-3+2x+x^2-y)}{x(3+x)y(3+y)}, \\
a_{8,5} &= -\frac{-9-x+x^2-3y-xy}{x(3+x)(3+y)}, a_{8,6} = -\frac{-3+2x+x^2-xy}{x(3+x)y}, \\
a_{8,8} &= \frac{9-6x-3x^2-6y-xy+x^2y-3y^2+xy^2+x^2y^2}{x(3+x)y(3+y)}, \\
a_{9,4} &= \frac{(1+y)(3-2x+y-xy)}{xy(3+y)}, a_{9,5} = \frac{(3-x+y)(1+y)}{xy(3+y)}, a_{9,8} = -\frac{1+y}{y(3+y)}, \\
a_{10,4} &= \frac{-2+3x-2y}{xy(3+y)}, a_{10,5} = -\frac{1-3x+2y+xy+y^2+xy^2}{xy(3+y)}, a_{10,8} = \frac{-1+y+xy}{xy(3+y)}, \\
a_{11,2} &= \frac{3}{x(3+x)y}, a_{11,4} = \frac{-9+5x+3x^2-3y-xy}{x(3+x)y(3+y)}, \\
a_{11,5} &= \frac{x-9y+x^2y-3y^2-xy^2}{x(3+x)y(3+y)}, a_{11,6} = -\frac{-x-3y+2xy+x^2y}{x(3+x)y}, \\
a_{11,8} &= -\frac{9-4x-3x^2-6y+2xy+x^2y-3y^2+2xy^2+x^2y^2}{x(3+x)y(3+y)},
\end{aligned}$$

where $x = \lambda_1 - \lambda_3$ and $y = \lambda_1 - \lambda_2$.

References

- [1] V.E. Korepin, N.M. Bogoliubov, and A.G. Izergin *Quantum inverse scattering method and correlation functions* (CUP, Cambridge, 1993).
- [2] M. Jimbo and T. Miwa, *Algebraic Analysis of Solvable Lattice Models* (AMS, Rhode Island, 1995).
- [3] M. Takahashi, J. Phys. C: Solid State Phys. **10** (1977) 1289.
- [4] M. Jimbo, K. Miki, T. Miwa and A. Nakayashiki, Phys. Lett. A **168** (1992) 256.
- [5] M. Jimbo and T. Miwa, J. Phys. A **29** (1996) 2923.
- [6] N. Kitanine, J. M. Maillet and V. Terras, Nucl. Phys. B **567** (2000) 554.
- [7] F. Göhmann, A. Klümper and A. Seel, J. Phys. A **38** (2005) 1833.
- [8] H. E. Boos and V. E. Korepin, J. Phys. A **34** (2001) 5311.
- [9] H. Boos, M. Jimbo, T. Miwa, F. Smirnov and Y. Takeyama, St Petersburg Math. J. **17** (2006) 85.
- [10] H. Boos, M. Jimbo, T. Miwa, F. Smirnov, Y. Takeyama, Comm. Math. Phys. **261** (2006) 245.
- [11] H. Boos, F. Göhmann, A. Klümper and J. Suzuki, J. Stat. Mech. (2006) P04001.
- [12] J. Damerau, F. Göhmann, N. P. Hasenclever and A. Klümper, J. Phys. A **40** (2007) 4439.

- [13] N. Kitanine, K. Kozlowski, J. M. Maillet, N. A. Slavnov and V. Terras, J. Stat. Mech. (2009) P04003.
- [14] Britta Aufgebauer and Andreas Klümper, J.Phys. A: Math. Theor. 45 (2012) 345203.
- [15] A. H. Bougourzi and R. A. Weston, Nucl. Phys. B **417** (1994) 439.
- [16] M. Idzumi, Int. J. Mod. Phys. A **9** (1994) 4449.
- [17] N. Kitanine, J. Phys. A **34** (2001) 8151.
- [18] T. Deguchi and C. Matsui, Nucl. Phys. B **831** (2010) 359.
- [19] F. Göhmann, A. Seel and J. Suzuki, J. Stat. Mech. (2010) P11011.
- [20] A. Klümper, D. Nawrath and J. Suzuki, J. Stat. Mech. (2013) P08009
- [21] G.A.P. Ribeiro and A. Klümper, J. Phys. A: Math. Theor. **49** (2016) 254001.
- [22] G. V. Uimin, JETP Lett. **12** (1970) 225.
- [23] B. Sutherland, Phys. Rev. B **12** (1975) 3795.
- [24] F. Göhmann, A. Klümper and A. Seel, J. Phys. A **37** (2004) 7625.
- [25] H.E. Boos, V.E. Korepin, F.A. Smirnov, Nucl.Phys. B **658** (2003) 417.
- [26] H.E. Boos, F. Göhmann, A. Klümper, J. Suzuki, J. Phys. A **40** (2007) 10699.
- [27] H.E. Boos, A. Hutsalyuk, K. Nirov, J. Phys. A: Math. Theor. 51 (2018) 445202 (arXiv:1804.09756 [hep-th]).